Pergamon

Prog. Oceanog. Vol. 34, pp. 285-334, 1994
Copyright © 1995 Elsevier Science Ltd
Printed in Great Britain. All rights reserved
0079 - 6611/94 $26.00

0079-6611(95)00001-1

The circulation and hydrography of the Marmara Sea

ŞÜKRÜ T. BEŞIKTEPE, HALIL İ. SUR, EMIN ÖZSOY, M. ABDUL LATIF, TEMEL OĞUZ and ÜMIT ÜNLÜATA

Institute of Marine Sciences, Middle East Technical University, PK 28 Erdemli, Içel, 33731, Turkey

Abstract – A comprehensive set of data collected during 1986-1992 reveal seasonal and interannual variability in the circulation and hydrography of the Marmara Sea. Waters, which have contrasting properties and originate from the adjacent basins, supply the two-layer stratified flows in the Sea of Marmara. Turbulent entrainment into the upper layer in the exit region of the Bosphorus jet, and wind-stirring in winter, both contribute equally to the basin vertical mixing.

The upper layer circulation of the Marmara Sea is determined from ADCP measurements and from dynamical calculations based on hydrographic data. The mean upper layer circulation is anti-cyclonic, mainly driven by the southward flowing Bosphorus jet in the enclosed domain. The Bosphorus inflow is well defined, except during the periods of low discharge in autumn and winter, when the jet becomes weaker and tends to become attached to the west coast near the exit.

Mediterranean waters, entering from the Dardanelles, supply the suhalocline layer. The negatively buoyant plume of well-oxygenated water is the only means of renewal of the deep waters, partially compensating for the oxygen consumed by the degradation of organic matter sinking from the upper layer into the lower layer. Yet the subhalocline waters remain permanently deficient in oxygen, as a result of the internal balances of diffusion, advection and consumption. The depth to which the plume penetrates is a function of the seasonal characteristics of the inflow density (modified in the Strait) and the weak interior stratification.

CONTENTS

1.	Introduction	286
2.	Regional characteristics	287
	2.1 Morphometry and Bottom Topography	287
	2.2 Meteorology	287
3.	The measurement program	290
4.	Exchanges with adjacent seas and the water budget	291
	4.1 Exchange flows through the Bosphorus and Dardanelles Straits	291
	4.2 The water budget and the steady-state fluxes	294
5.	Upper layer hydrographic variability and mixing characteristics	297
	5.1 Water masses and their seasonal variability	297
	5.2 Upper layer mixing in transit through the system	297
	5.3 Interannual and long-term changes	302
	5.4 Impacts on environmental health	305
6.	Upper layer circulation	305
	6.1 Seasonal circulation	305
	6.2 The Bosphorus jet	310
7.	Hydrographic variability of the subhalocline water masses	310
	7.1 Water masses	310
	7.2 Renewals of the subhalocline waters	310
	7.2.1 Seasonal variability	315
	7.2.2 Interannual variability	319
	7.2.3 Ventilation	323
	7.3 Interior mixing	326
	7.4 Circulation characteristics of the subhalocline waters	326
	7.5 Outflow of the sub-halocline waters	329
8.	Summary and conclusions	330
9.	Acknowledgements	332
10.	References	332

1. INTRODUCTION

The hydrography of the Marmara Sea has been known in outline since the expedition of NIELSEN (1912). Since this early work, further studies of the Marmara Sea have been carried out by MÖLLER (1928), PEKTAS (1953) and ARTÜZ (1974), which served to define general characteristics of the water masses and the circulation of the basin. Recent measurements carried out by the Institute of Marine Sciences (IMS-METU) have either added considerable detail or changed some of the interpretations of the early results (ÖZSOY, OĞUZ, LATIF and ÜNLÜATA, 1986; ÖZSOY, OĞUZ, LATIF, ÜNLÜATA, SUR and BEŞİKTEPE, 1988; LATIF, OĞUZ, SUR, BEŞİKTEPE, ÖZSOY and ÜNLÜATA, 1990; ÜNLÜATA, OĞUZ, LATIF and ÖZSOY, 1990).

The hydrography of the Marmara Sea is essentially determined by the exchange through the Straits. A sharp density interface ($\Delta\rho/\rho \approx 10^{-2}$), at a depth of ~25m separates the two distinct water types originating from the adjoining basins, i.e. the low salinity ($S \approx 18$ppt) waters of the Black Sea entering from the Bosphorus and the salty ($S \approx 38$ppt) waters of the Mediterranean entering from the Dardanelles. The strong pycnocline inhibits mixing between the two layers. However considerable mixing occurs, especially in winter, as a result of wind stirring (ANDERSON and CARMACK, 1974). Turbulent entrainment processes account for the exchange between the layers (ÜNLÜATA, OĞUZ, LATIF and ÖZSOY, 1990), resulting in a lengthwide variation of salinity in the upper layer. The most important contribution to entrainment into the upper layer occurs in the region where the Bosphorus inflow into Marmara takes the form of a jet issuing into the upper layer.

In this paper we examine the features of the hydrography and circulation of the basin throughout the measurements carried out by the IMS-METU on a seasonal basis between 1986 and 1992. Section 2 presents a brief review of the regional characteristics. Section 3 presents a description of the data set and the methods used. Section 4 discusses the exchanges of water masses with the adjacent seas. Section 5 presents the hydrography of the upper layer. Section 6 discusses the upper layer circulation. Section 7 concentrates on the sub-halocline part of the basin with emphasis on the temporal and spatial variability of the water masses and circulation.

2. REGIONAL CHARACTERISTICS

2.1 Morphometry and bottom topography

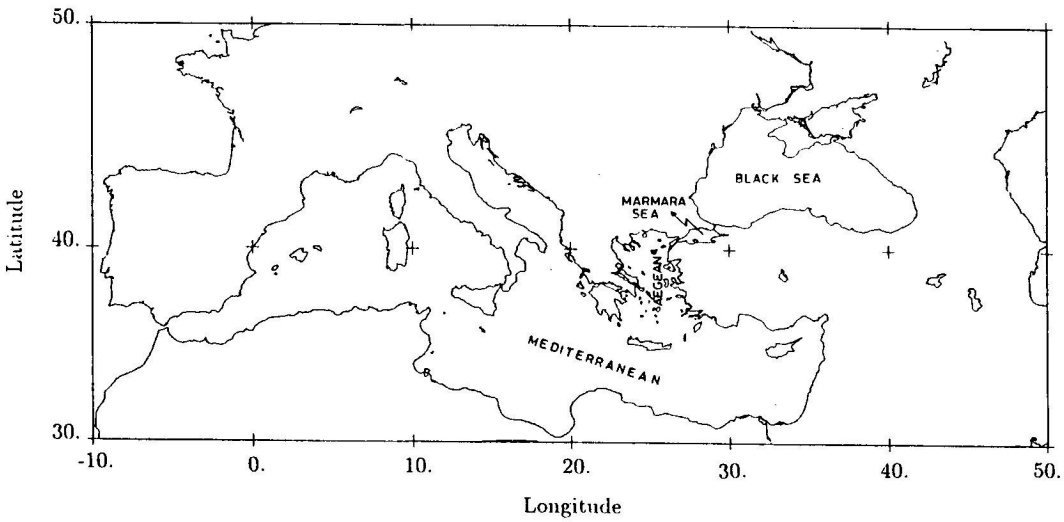
The Sea of Marmara is a small basin (size: ~70km x 250km, surface area: 11500km^2, maximum depth 1390m) located between the continents of Europe and Asia, and connecting with the Mediterranean Sea and the Black Sea (Fig.1a) respectively through the Dardanelles (length: ~60km, width: ~1.3-7.0km)) and the Bosphorus (length: ~30km, width: ~0.7-3.5km) Straits. The Straits and the Marmara Sea together constitute the Turkish Straits System.

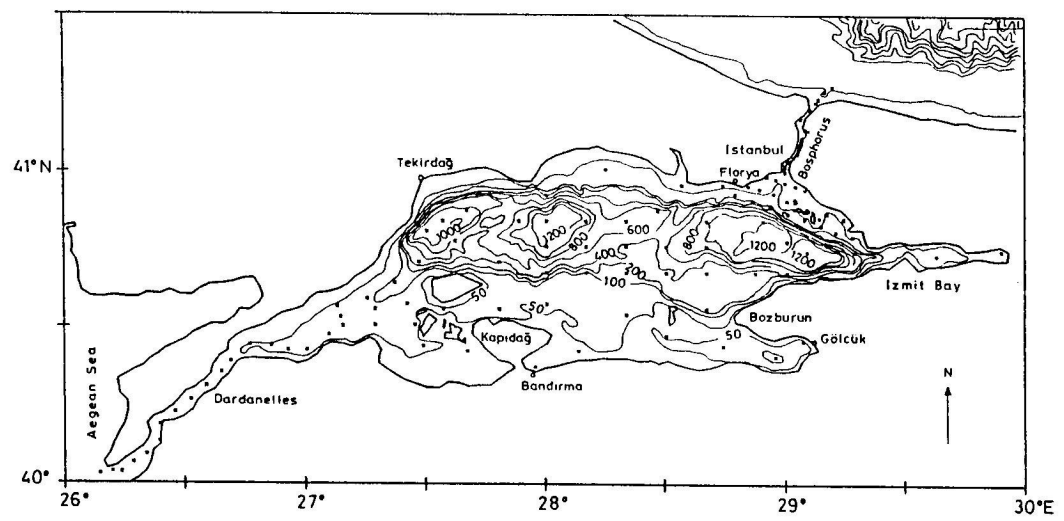
The three topographic depressions in the northern part of the Marmara Sea are seaward extensions of the well known North Anatolian Fault Zone spanning the Anatolian peninsula (Fig.1b). Of these, the eastern basin (maximum depth ≈ 1240m) has been characterized as a pull-apart basin, while the central and western basins (with respective depths of 1389m and 1097m) have been characterized as compressional depressions (SENGÖR, GÖRÜR and SAROĞLU, 1985). The sills connecting each pair of basins have depths of ~750m; the eastern sill has a length of ~40km, and the western sill has a length of ~20km. The continental shelf bordering the southern margin of the basin is shallow (~100m) and wide (~30km), whereas the shelf along the north coast is extremely narrow (<10km), and its only relatively wide region is in the triangular entrance region of the Bosphorus.

The Dardanelles Strait joins the Marmara Sea through a funnel-shaped extension which gradually widens eastwards. Within this funnel region is a narrow groove (maximum depth ~70m) in the bottom topography which extends east from the narrowest section of the Strait, connecting it to the flat southern shelf region of the Marmara Sea (Fig.1c). Beyond the end of this channel, the bottom topography slopes gently towards the western depression until the incline steepens sharply into a small canyon.

2.2 Meteorology

The moderate wind climate of the Marmara region is strongly influenced by land topography. The entire region of low-lying topography surrounding the Turkish Straits System is a passageway for cold wind systems from the north, and for cyclones moving from the Aegean into the Black Sea (BRODY and NESTOR, 1980). The topographies of the valleys of the Bosphorus and Izmit Bay locally influence wind direction and speed. Northeasterly winds are prevalent throughout the year, with an average frequency of 60%, and southwesterly winds are of secondary importance (20%). The daily average wind speed is 4ms^{-1}. Strong wind events with typical speeds of 8-25ms^{-1} and durations of about 16 hours occur in winter, especially near the Bosphorus junction (DE FILIPPI, IOVENITTI and AKYARLI, 1986). Moderate northeasterly and southeasterly winds are common during summer.


50.
40.
30.
Latitude
-10.
0.
10.
20.
30.
40.
50.
Longitude
BLACK SEA
MARMARA SEA
AEGEAN SEA
MEDITERRANEAN


41°N
40°
26°
27°
28°
29°
30°E
Tekirdağ
Istanbul
Florya
Bosphorus
İzmit Bay
Bozburun
Gölcük
Kapıdağ
Bandırma
Dardanelles
Aegean Sea
N
50
100
300
400
600
800
1000
1200

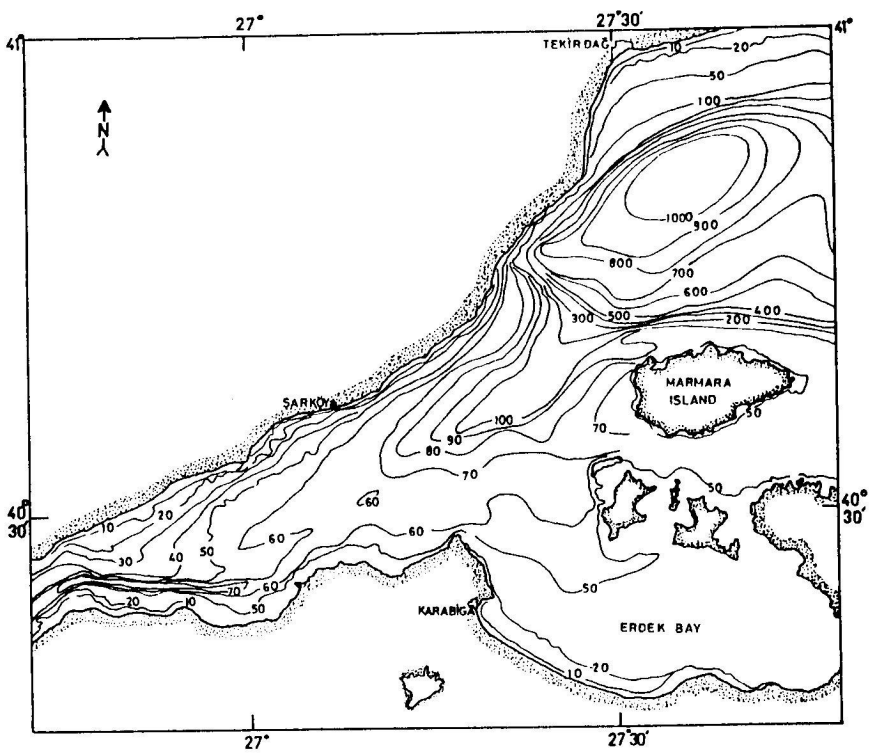


FIG. 1. (left and above) Regional maps showing (a) the location and (b) the bathymetry of the Marmara Sea (Station positions corresponding to Fig.2 are superimposed); (c) detailed bathymetry of the Dardanelles-Marmara junction region. Depth contours are labelled in metres.

The air temperature is coldest and precipitation highest during January. Warmest temperatures coincide with minimum precipitation during July. The sea surface temperature follows the air temperature with a lag of about one month reaching a minimum in February, and a maximum in August (BEŞIKTEPE, 1991).

3. THE MEASUREMENT PROGRAM

The CTD data were collected during a series of cruises (Table 1) by the *R/V Bilim*, the research vessel of the IMS-METU, as part of a long-term observational program (ÖZSOY, OĞUZ, LATIF and ÜNLÜATA, 1986; ÖZSOY, OĞUZ, LATIF, ÜNLÜATA, SUR and BEŞIKTEPE, 1988; LATIF, ÖZSOY, OĞUZ and ÜNLÜATA, 1991). A typical station grid is shown in Fig.2. An additional network of stations (not shown) was visited more frequently within the Straits and their junctions with the Marmara Sea.

TABLE 1: Data summary

Cruise	Date	Number of Stations
March 1986	13-19 March 1986	44
April 1986	25 April - 6 May 1986	42
July 1986	7-8 July 1986	21
November 1986	19-27 November 1986	57
February 1987	30 January - 6 February 1987	49
March 1987	31 March - 1 April 1987	14
May 1987	15-21 May 1987	70
August 1987	11-16 August 1987	70
March 1988	19-27 March 1988	83
July 1988	3-11 July 1988	82
September 1988	20-25 September 1988	67
December 1988	13-15 December 1988	40
February 1989	14-18 February 1989	71
March 1989	20-24 March 1989	74
September 1989	19-26 September 1989	80
March 1990	8-12 March 1990	91
May 1990	4-8 May 1990	93
July 1990	27 July - 1 August 1990	82
October 1990	25-30 October 1990	75
January 1991	11-18 January 1991	75
June 1991	19-22 June 1991	87
October 1991	1-7 October 1991	18
March 1992	8-21 March 1992	90
October 1992	15-19 October 1992	90

A Sea Bird Electronics SBE 9 CTD profiler equipped with pressure, temperature, conductivity and oxygen sensors was used for the measurements. Regular calibrations were not undertaken, but interseasonal comparisons based on the stable deep water characteristics elsewhere indicated that seasonal drifts were limited to ±0.03°C for temperature and ±0.04ppt for salinity (BEŞIKTEPE, 1991), within the limits of the manufacturer's specifications.

The density distribution was used in dynamic computations of the upper layer circulation, although a geostrophic balance was not expected to be particularly well suited for a small inland sea with extensive shallow regions. However, comparison with simultaneous ADCP data during the later phases of the observational program indicated reasonable agreement with the dynamic computations. The lower layer is essentially motionless, and so the upper layer dynamic computations were insensitive to the choice of the level of no motion, as long as this level was deeper than the halocline (depth >25m). Based on sensitivity studies confirming this result (BEŞIKTEPE, 1991), a reference layer of 100m depth was selected.

The geostrophic computations are least applicable to the region of the Bosphorus inflow, which is governed by non-linear and dissipative dynamics. Surprisingly, though, even during the peak

inflow conditions, i.e. the spring and summer months, our dynamic computations seem to produce realistic looking inflow streamlines for this region.

The current data were collected with an RD Instruments 150 KHz vessel-mounted ADCP with up to 128 depth bins extending to a maximum depth of about 200m. The data were collected both at hydrographic stations and while the ship was under way, with an ensemble averaging period of at least five minutes. Absolute velocity values were calculated either with the bottom tracking option in those regions where depths were shallower than 350m, or relative to a reference layer of 50-100m in the deeper areas.

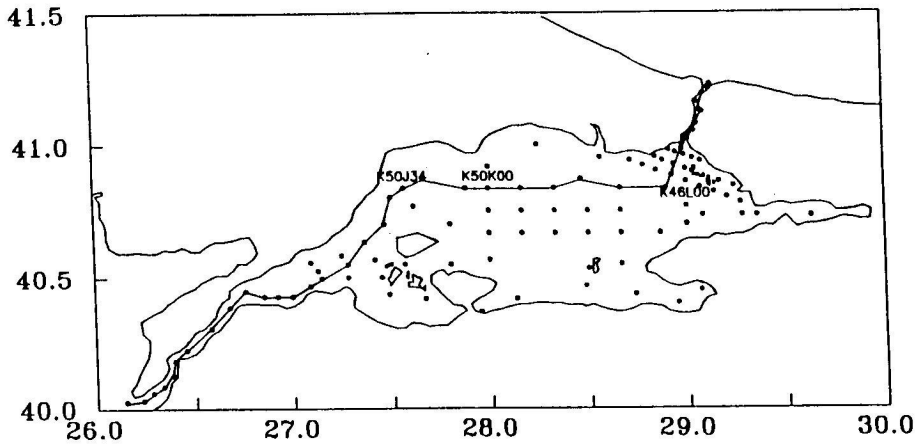


FIG.2. A sample of the station network used during this study. Three main stations mentioned in the text are labelled. Also shown is the location of the transect along the main axis of the Marmara Sea.

4. EXCHANGES WITH ADJACENT SEAS AND THE WATER BUDGET

4.1 Exchange flows through the Bosphorus and Dardanelles Straits

Flows through the Turkish Straits are driven by the density differences between the Black Sea and the Aegean, and maintain a net sea level difference between these seas. Based on data for the 1946-56 period, BOGDANOVA (1969) estimated the mean sea level difference between the Black Sea and the Aegean Sea to be 42cm, with seasonal changes reaching a minimum of 35cm in October and a maximum of 57cm in June, corresponding to the periods of minimum and maximum fluxes respectively from the Black Sea. Reviewing recent sea-level data, BÜYÜKAY (1989) found a mean sea-level difference of about 30cm between the two ends of the Bosphorus, with smaller seasonal differences (of ±10cm). Recent studies (ÖZSOY, OĞUZ, LATIF and ÜNLÜATA, 1986; ÜNLÜATA, OĞUZ, LATIF and ÖZSOY, 1990) have shown that there are two hydraulic controls, imposed at the mid-strait contraction section and at the northern sill. Combined with suitable reservoir conditions, the flow transitions at these controls make the Bosphorus the foremost example of a strait with *maximal exchange* (FARMER and ARMI, 1986; ARMI and FARMER, 1987), implying that the Strait dynamics determine the exchange between the adjacent basins. Following a hydraulic jump south of the constriction, a third flow transition of secondary importance occurs at the southern end of the Bosphorus. Numerical model studies (OĞUZ, ÖZSOY, LATIF, SUR and ÜNLÜATA, 1990) have confirmed these basic results and have established the relationship between the flux components as functions of forcing, and the internal parameters of the Strait. The particular setting of the Bosphorus, with the sill located near the smaller density basin, yields nonlinear flow assymmetries

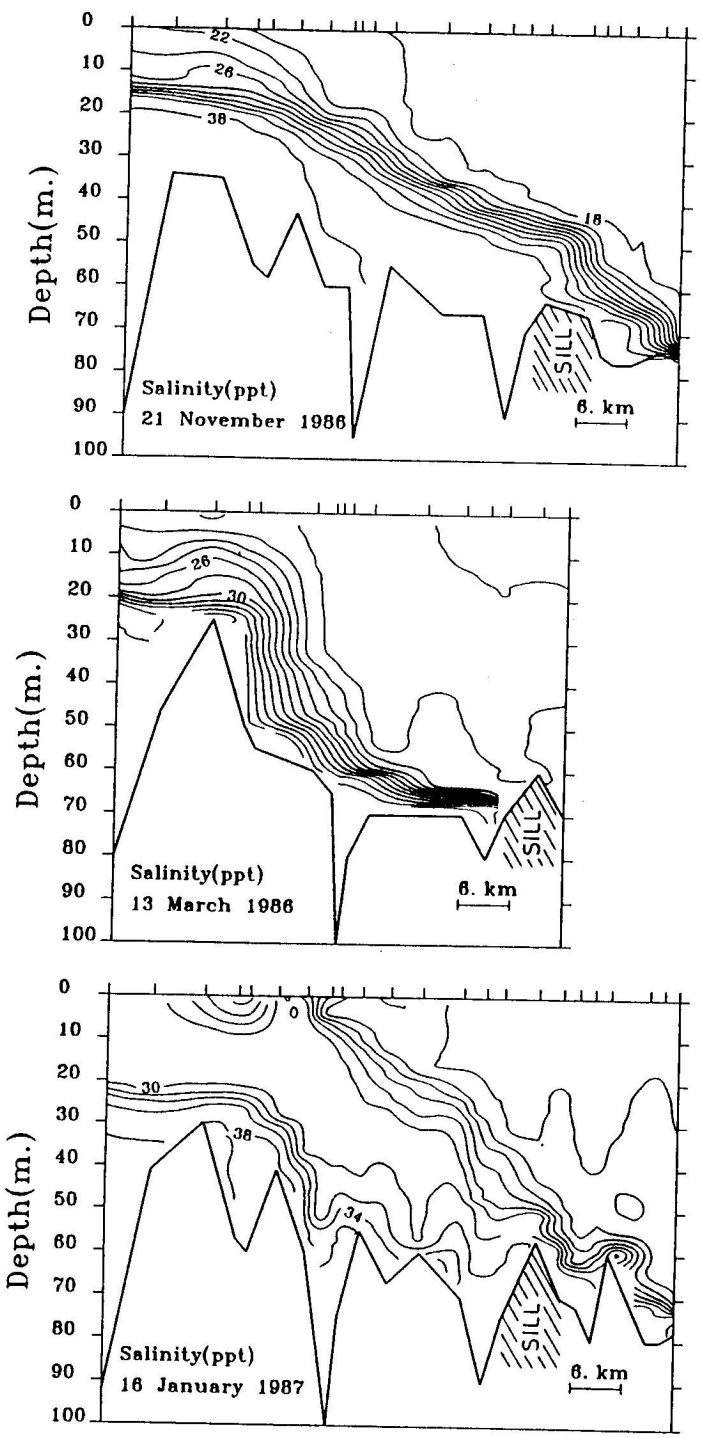


FIG. 3. The salinity distribution in the Bosphorus: (a) 'normal' two layer exchange; (b) lower layer flow blocked at the northern sill; and (c) upper layer blocked, with resulting three layers (after LATIF, ÖZSOY, OĞUZ and ÜNLÜATA, 1991).

with respect to net through-flow and control section geometry (FARMER and ARMI, 1986), resulting in substantial variability in flow. A hydraulics model including these effects and time dependent storage in the Black Sea is able to reproduce seasonal changes in response to the water budget (ÖZSOY, 1990; ÖZSOY, LATIF, TUĞRUL and ÜNLÜATA (1992a) and SUR, ÖZSOY and ÜNLÜATA (1994), noted a correlation between the Danube river inflow and the Black Sea mean sea-level on interannual time scales.

The Bosphorus operates in the full range of weak to strong barotropic forcing in either direction (Figs 3a-c). Blocking of the flows in either layer occurs during extreme events, which can last for a few days. The lower layer blocking typically occurs during the spring and summer months, when the net freshwater influx into the Black Sea increases (Fig.3b). The upper layer blocking events (identified locally as *Orkoz*), occur in the autumn and winter months, when the surface flow reverses (Fig.3c). These events were detected during the frequent hydrographic surveys (ÖZSOY, OĞUZ, LATIF and ÜNLÜATA, 1986; LATIF, ÖZSOY, OĞUZ and ÜNLÜATA, 1991) and were verified by continuous current-meter and Acoustic Doppler Current Profiler (ADCP) measurements in the Bosphorus (LATIF, ÖZSOY, SALİHOĞLU, GAINES, BAŞTÜRK, YILMAZ and TUĞRUL, 1992b; ÖZSOY, LATİF, TUĞRUL and ÜNLÜATA, 1992a; ÖZSOY, LATIF, BEŞİKTEPE, OĞUZ, SALİHOĞLU, GAINES, TUĞRUL, BAŞTÜRK, SAYDAM, YEMENİCİOĞLU and YILMAZ, 1992b). Although seasonal changes are evident in the data, it is the short term transients response to meteorological events which are overwhelmingly dominant as revealed by ADCP-based flux computations (Fig.4).

The flow regime of the Dardanelles Strait differs from that of the Bosphorus. A single hydraulic control section at the mid-Strait constriction results in submaximal exchange (ÖZSOY, OĞUZ, LATIF and ÜNLÜATA, 1986; OĞUZ and SUR, 1989). Although the exchange can be idealized as consisting of two-layers, the relatively wider and deeper channel of this strait allows not only density stratification but also reversals of flow within the lower layer.

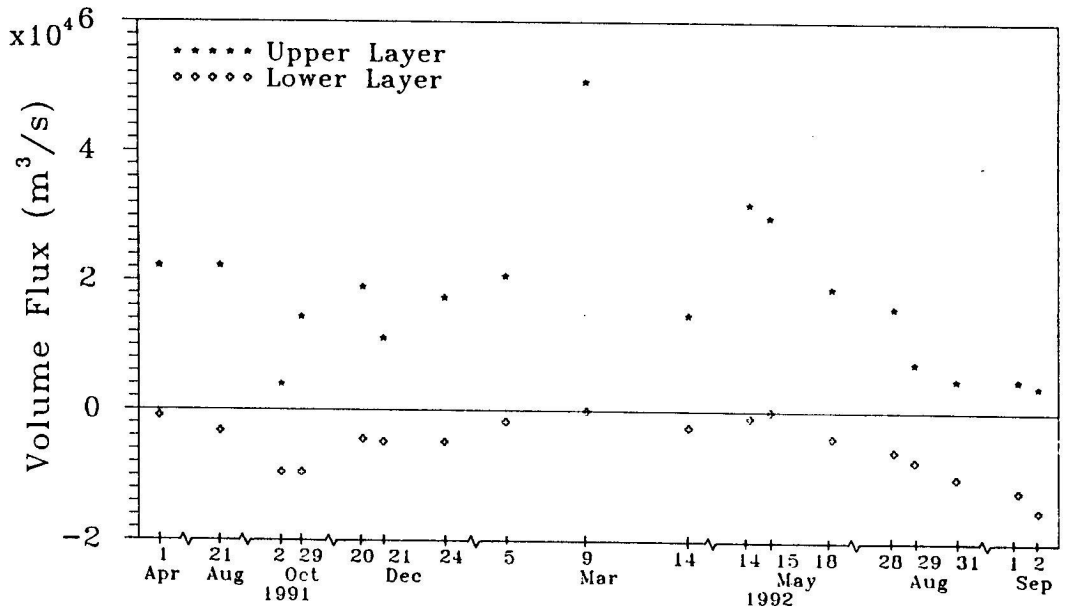


Fig.4. Volume flux computations based on ADCP measurements in the Bosphorus during different experiments between 1991-1992. The dates of the measurements are placed along the horizontal axis. Positive indicate northward. The data taken from ÖZSOY, LATIF, TUĞRUL and ÜNLÜATA (1992).

4.2 The water budget and the steady-state fluxes

The two-layer flows through the Bosphorus (the exchange flows to and from the Black Sea) have been estimated in various literature sources. A critical review and improved estimates of fluxes have been given by ÜNLÜATA, OĞUZ, LATIF and ÖZSOY (1990).

The flux computations are based on the Knudsen relations expressing the steady-state mass budgets. For each compartment of the system displayed in Fig.5, water and salt conservation are stated as:

$$Q_{1o} + Q_d = Q_{1i} + Q_f + Q_u$$

$$Q_{2o} + Q_u = Q_{2i} + Q_d$$

$$S_{1o}Q_{1o} + S_1Q_d = S_{1i}Q_{1i} + S_2Q_u$$

$$S_{2o}Q_{2o} + S_2Q_u = S_{2i}Q_{2i} + S_1Q_d$$

The fluxes entering and leaving the upper layer (Q_{1i}, Q_{1o}), those entering and leaving the lower layer (Q_{2i}, Q_{2o}), and those entrained in the upper and lower layers (Q_u, Q_d), respectively, can be determined from the above equations, if the net fresh water inflow ($Q_f + Q_p + Q_4 - Q_e$ (where Q_p, Q_r and Q_e are the precipitation, runoff and evaporation fluxes) is specified at the surface, and the salinities S_{1i}, S_{1o}, S_{2i}, S_{2o}, S_1, S_2 are specified at the two ends of each compartment and for each layer. Note, however, that this system is indeterminate in each separate compartment, because it involves six unknowns and four equations. We can close the system at the Black Sea, a semi-enclosed sea, by setting $Q_{1i} = 0$ and $Q_{2o} = 0$ at this end.

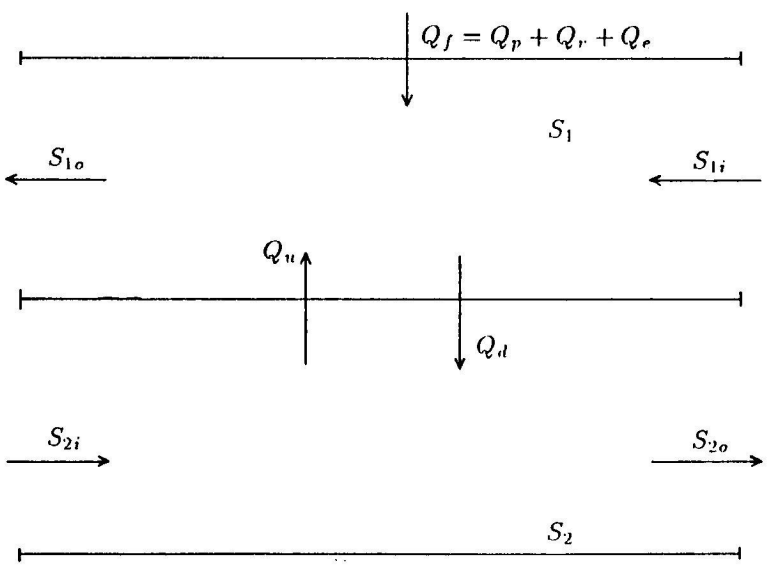


FIG.5. Compartment flows in a two-layer system.

For reliable estimates of steady fluxes, long-term average values of salinity were computed at the strait entrances. Since local definitions were needed for the layers, the salinity values $S_1^* = S_s + 0.2(S_b - S_s)$ and $S_2^* = S_b - 0.2(S_b - S_s)$ were assigned as the salinity limits characterising the upper and lower layer waters respectively, where S_s is surface salinity (averaged for the first 5m) and S_b the bottom salinity (averaged within 5m from the maximum depth of each cast). The salinity values $S < S_1^*$ and $S > S_2^*$ were then averaged to compute average upper and lower layer salinities, S_1 and S_2, respectively.

The salinity and flux computations were updated several times, based on data accumulated between 1986-1991 (ÖSZOY, OĞUZ, LATIF and ÜNLÜATA, 1986; ÖZSOY, OĞUZ, LATIF, ÜNLÜATA, SUR and BEŞIKTEPE, 1988; LATIF, OĞUZ, SUR, BEŞIKTEPE, ÖZSOY and ÜNLÜATA, 1990; BEŞIKTEPE, 1991), with an earlier version given by ÜNLÜATA, OĞUZ, LATIF and ÖZSOY (1990). The most recent update is given in Fig.6.

In the Black Sea, the contributions of precipitation and river runoff are approximately equal in magnitude (300 and 350km^{3}y^{-1} respectively), giving a total fresh water input about twice that of the loss by evaporation (350km^{3}y^{-1}). The average fluxes at the Black Sea end of the Bosphorus (Fig.6) are computed to be Q_{1b}=600km^{3}y^{-1} (outflowing from the Black Sea) and Q_{2b}=300km^{3}y^{-1} (inflowing into the Black Sea) respectively. The budget of the Black Sea requires that the ratio $Q_{1b}/Q_{2b} = S_{2b}/S_{1b} = 35.5/17.9 \approx 2$, where Q_{1b}, S_{1b} and Q_{2b}, S_{2b} are the upper and lower layer volume fluxes and salinities defined at the Black Sea entrance of the Bosphorus. Approximately 650km$_3$y^{-1} of Black Sea water enters the Marmara Sea from the Bosphorus, and 550km^{3}y^{-1} of Mediterranean water enters from the Dardanelles.

In the Bosphorus, about 25% of the Mediterranean water influx is entrained into the upper layer, and about 7% of the Black Sea water is entrained into the lower layer flow. The computations show that 45% of the Aegean inflow is entrained into the upper layer in the Dardanelles; a further 45% of the amount reaching the Marmara Sea is lost to the upper layer by basin-wide entrainment.

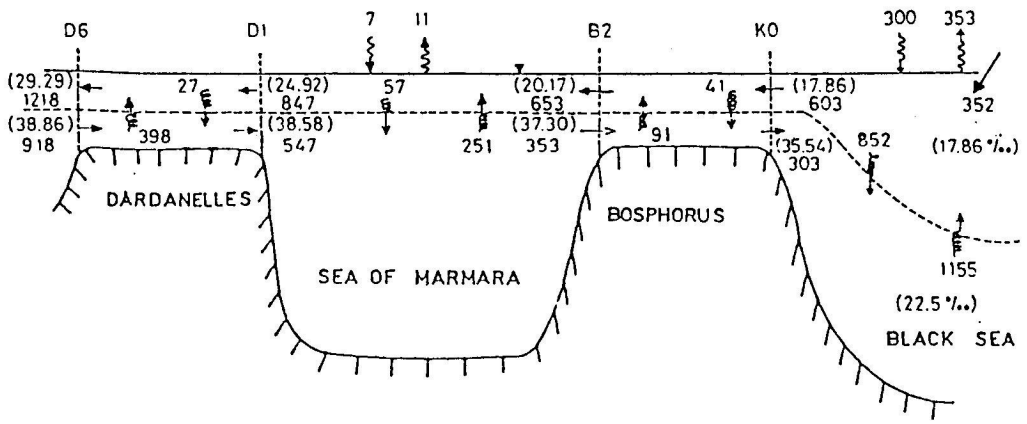


FIG.6. Volume fluxes across the compartments of the Turkish Straits System using 4yr (1986-1989) average salinities. The fluxes are given in units of km^{3}y^{-1} (1km^{3}y^{-1} = 31.7m^{3}s^{-1}). Numbers in parentheses are average salinity values used in the computations.

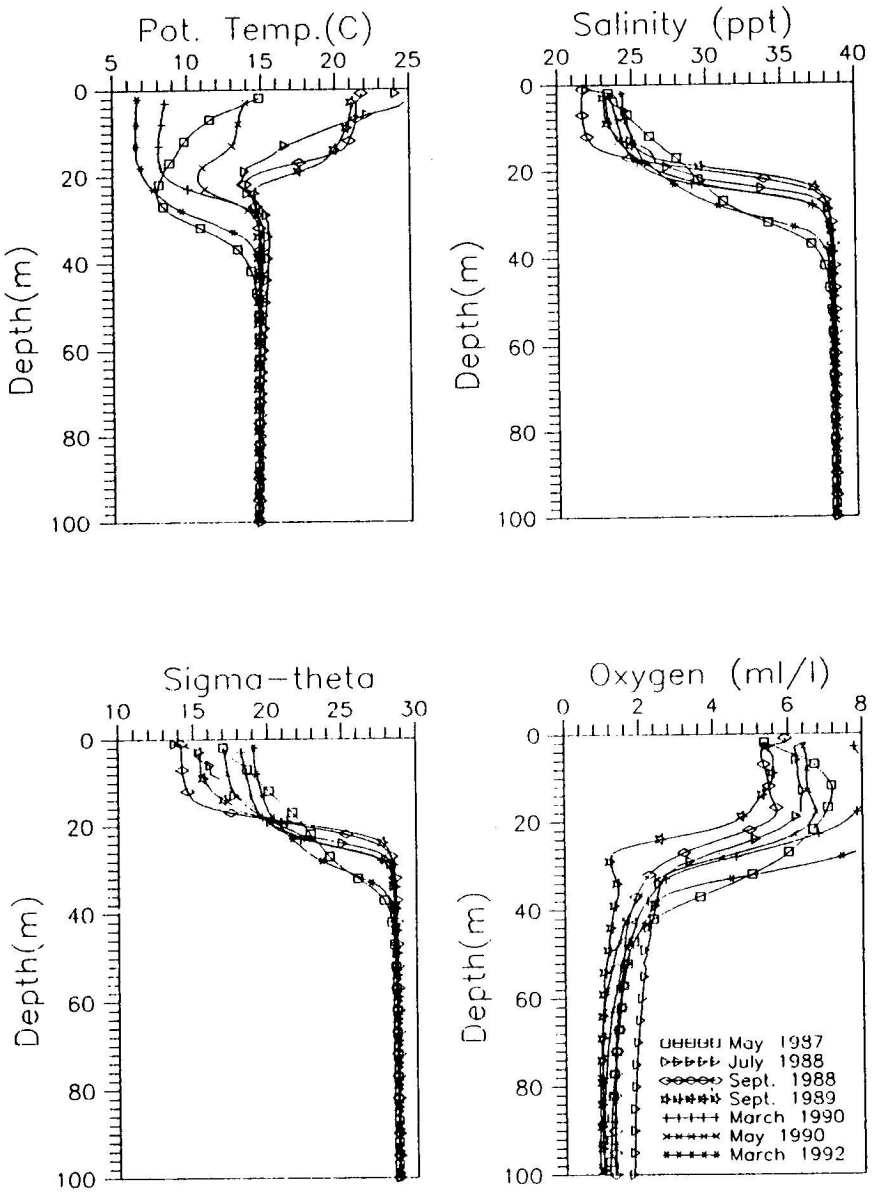


FIG.7. Cruise averaged (a) potential temperature (b) salinity (c) sigma-theta (d) oxygen profiles for the upper 100m of the basin for ten different months.

5. UPPER LAYER HYDROGRAPHIC VARIABILITY AND MIXING CHARACTERISTICS

5.1 Water masses and their seasonal variability

The upper layer waters largely reflect the seasonal characteristics of Black Sea water modified in transit through the Bosphorus, and by local heating/cooling and mixing in the Sea of Marmara. The seasonal variability in the upper layer is illustrated in Fig.7, where basin averaged vertical profiles of potential temperature (θ), salinity, density (σ_θ), and dissolved oxygen are displayed. Seasonal variations are essentially confined to the well aerated upper layer (depth <25m), but extreme wind mixing events, such as in May 1987, are able to erode the halocline down to a depth of about 40m.

Spring-time solar heating warms the water in the upper 15m. There is a residual Cold Intermediate Layer (CIL) at the halocline, analogous to the CIL in the Black Sea, which results from advection via Bosphorus as well as local winter cooling in Marmara (ÖZSOY, OĞUZ, LATIF and ÜNLÜATA, 1986). The CIL persists through most of the year with a minimum temperature of 8°C, and has its highest contrast with surface temperatures in the spring and summer.

The upper layer salinity is in the range of 23 ± 2ppt, reaching a maximum in winter, as a result of increased wind mixing in the basin and reduction in the influx from the Black Sea. Erosion of the halocline during the winter can broaden it, in contrast to its usual sharp interface at other times, as shown in the exceptional case of May 1987. The oxygen profiles in the upper layer reflect largely the effect of temperature on the solubility of oxygen in seawater, with an increase at the Cold Intermediate Layer. The oxygen saturation ratio in the upper layer is in the range of 0.7-1.5.

5.2 Upper layer mixing in transit through the system

Infrared and visible satellite images of the Marmara Sea (Figs 8a,b) illustrate the main features of its circulation and the evolution of the characteristics of the upper layer waters in transit. During typical flow conditions in the spring and summer, the relatively colder Black Sea waters enter the Marmara Sea in the form of a jet which extends as far as the Bozburun peninsula in the south, before it turns west and northwest to reach the Thracian coast and then exits towards the Dardanelles.

Surface salinity distribution (at 5m depth) displayed in Figs 9a,b indicate the same features. Black Sea water entering the Marmara Sea has a salinity of about 19-21ppt which becomes 22-25ppt by the time it enters the Dardanelles. Low salinities can be followed from the entrance region of the jet to where they reach Bozburun Peninsula on the opposite coast. Most of this core of low salinity then turns toward the northwest, but a smaller part occasionally moves towards Izmit Bay. The salinity increases in the sheltered Bays of Gemlik and Izmit to the east of the Bosphorus jet, and to the west of the Kapidag peninsula away from the low salinity core exiting the system along the northern coast.

In Fig.10, the upper layer average salinity is plotted versus distance for observations exemplifying the seasonal changes in mixing. Since the water properties within each layer change along the system, the limiting and average salinity for the upper layer have been determined locally using the techniques outlined in Section 4.2.

The maximum surface salinities occur in winter, February and March, when wind-stirring has its largest influence (Fig.10). The example of February 1987 shows an extreme event, not repeated during the total period of the observations. The mean upper layer salinity decreases during summer when the inflow of fresher water from the Black Sea increases.

A lag in the seasonal response of the system (proportional to an upper layer residence time of four months) is evident in the salinity distributions, reflecting the effects of waters introduced into

the system during the earlier seasons. For example, the effects of winter mixing in February 1987 persisted until May 1987 in the western basin (Fig.10), despite the increase in Bosphorus discharge during spring. Surface salinity remained high (~27ppt) in the western basin, but decreased sharply to (~23ppt) in the eastern basin as a result of the influx of low salinity waters from the Bosphorus. The same effects are evident in Fig.9a. Lower and more uniform salinity values were observed during the following survey of August 1987 (Fig.10). Even lower salinities (21-22.5ppt) were observed in the autumn season of the following year (September 1988), see Fig.9b.

In both cases illustrated in Figs 9a,b, water entering the Bosphorus from the Black Sea had a salinity of about 17-18ppt, which had increased to about 19-20ppt at the southern exit of the Bosphorus, where the dissipative hydraulics of the region to the south of the Strait's constriction resulted in entrainment of the Mediterranean water from the lower layer. When the Bosphorus jet enters the Marmara Sea, there is a further increase of salinity (to 21-22ppt) in the junction region as a result of jet mixing, i.e. there is lateral entrainment of the ambient Marmara waters along the jet and vertical entrainment of Mediterranean water from the underlying lower layer.

More generally, the mixing-evolution of the conservative properties of the upper layer in transit through the Turkish Straits System is determined by two basic processes: (i) mixing laterally along the jet boundaries within the dissipative flow transition regions of the Straits and jet mixing in the exit regions, e.g. the southern Bosphorus hydraulic transition and Marmara junction jet entrainment (similar results apply for the Dardanelles Strait in the flow transition downstream of its constriction at Nara, and at its exit region to the Aegean, see ÖZSOY, OĞUZ, LATIF and ÜNLÜATA, 1986; OĞUZ and SUR, 1989); and (ii) the basin-wide turbulent entrainment of the lower layer waters into the upper layer. Although the latter kind of entrainment includes a wide range of turbulence time scales of fluctuating currents and waves acting over the basin domain, its most important component is wind-stirring. In winter, the upper layer in the entire Marmara becomes well mixed, and its total depth and salinity are increased by mixing with the underlying Mediterranean waters (BEŞİKTEPE, ÖZSOY and ÜNLÜATA, 1993). In Figs 9 and 10 we observe that both of the above processes are equally important, with comparable effects on upper layer salinity: the salinity increase at the entrance region of the Bosphorus at any time is of the same magnitude as the difference between winter and summer salinities in the Marmara Sea. Based on steady-state mass and salt balances at the inflow and outflow sections, it is estimated that about $250 km^3 y^{-1}$ of lower layer waters are entrained annually into the upper layer (Section 4.2). This estimate includes the net effect of various forms of turbulent entrainment acting throughout the basin, including wind stirring, integrated contributions of meso-scale time-dependent motions, and the turbulent entrainment by the Bosphorus jet.

The wind induced entrainment component can be estimated from bulk formulae for given wind stress values and the characteristic stratification. For example, the entrainment velocity into the upper layer can be estimated from the following empirical formula for wind driven entrainment velocity in two layer flows (BO PEDERSEN, 1980):

$$\frac{v_e}{u_*} = \frac{2.3}{6+Ri_f},$$

where we define the bulk Richardson number $Ri_f = g'h/u_*^2$, the friction velocity $u_* = \sqrt{\tau_w/\rho}$, the wind stress $\tau_w = \rho_a C_d u_w^2$, where ρ is the water density, $g' = g\Delta\rho/\rho$ the reduced gravity, h the upper layer depth, C_d the drag coefficient, u_w is the wind velocity, and ρ_a the air density.

A rough estimate of the wind induced entrainment can be found from the above. Assuming average wind velocities of $8 ms^{-1}$ for winter and $4 ms^{-1}$ for the remaining part of the year, taking $\rho_a = 1.22 kgm^{-3}$, $C_d = 0.0012$ and $\rho = 1018 kgm^{-3}$, $\Delta\rho/\rho = 0.01$, and using $A = 11500 km^2$ for the surface



FIG.8. (a) Infrared image of the Marmara Sea taken by NOAA-10 on August 1990. The lighter tones represent warmer water and the darker tones represent colder water. (b) (overleaf) Visible image of the Marmara Sea taken by SKYLAB.



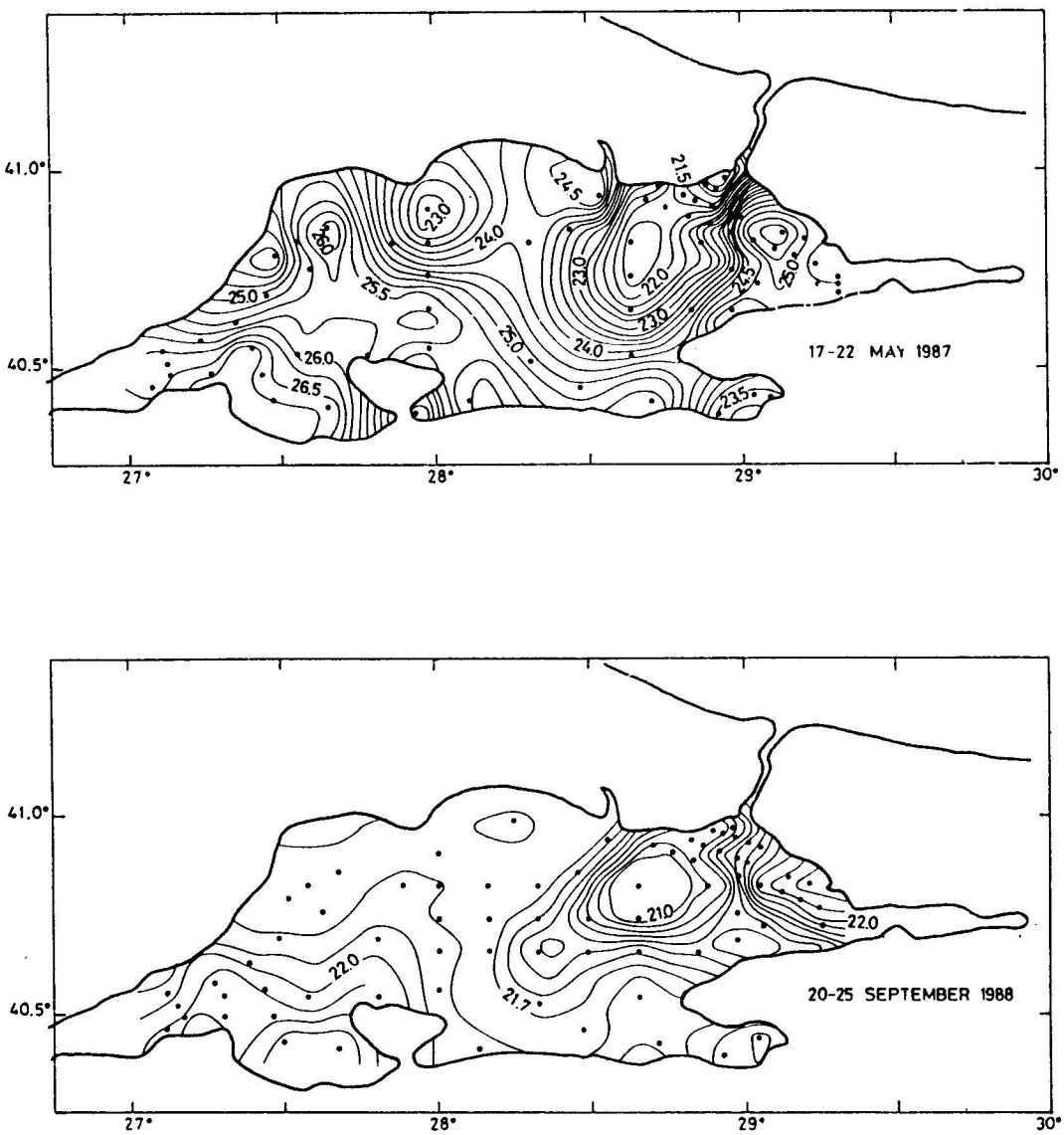


FIG.9. Distribution of surface salinity in the Marmara Sea for (a) May 1987 (b) September 1988.

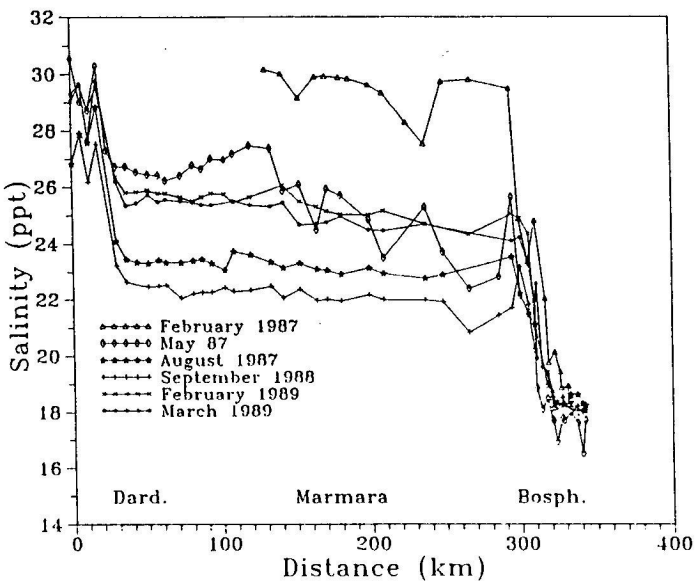


FIG.10. Upper layer averaged salinity distribution along the main axis of the Turkish Straits System for different months.

area of the basin, the entrainment flux is calculated to be $Q_e = v_e A = 118 km^3 y^{-1}$, corresponding to less than half of the total upward volume flux at the interface. About $86 km^3 y^{-1}$ of this flux corresponds to winter, and $32 km^3 y^{-1}$ occurs during the rest of the year. The remaining part of the upward flux should be accounted for by the jet entrainment at the Bosphorus junction.

5.3 Interannual and long-term changes

Interannual changes are common in the Turkish Straits System, which is situated between two large basins much affected by climatic fluctuations. Its oceanography is largely determined by the prevailing conditions in the adjacent basins, whose atmospheric forcing has much in common and so the Turkish Straits System responds sensitively to such changes.

For example, the fresh water inflow into the Black Sea is subject to large seasonal and interannual variations; the seasonal discharges of large rivers (e.g. the Danube) vary by a factor of 3 between the minimum and maximum values (SUR, ÖZSOY, and ÜNLÜATA, 1993). More significantly, the changes in fresh water influx seem to result in interannual sea-level fluctuation in the Black Sea (Section 4.1), which are modulated by the flows through the Turkish Straits.

Salinity measurements imply that low salinity waters generated by the discharges of major rivers in the northwestern Black Sea reach the southwest coast. Minimum salinities are observed in the March-August period, but are subject to significant differences in the timing and value from one year to the next (SUR, ÖZSOY, and ÜNLÜATA, 1994).

Long-term variations are evident in records of sea surface temperature at several stations in the Marmara region, with strong correlations between the minimum and maximum temperatures observed at the different stations (Fig.11, ÖZSOY, OĞUZ, LATIF and ÜNLÜATA, 1986). Extreme cold temperatures of 3°C were observed at Florya during the winters of 1944 and 1954. Waters of ~2°C were observed along the Black Sea entrance at Kumköy during 1954, at the same time that ice floes reached the Bosphorus from the north (ACARA, 1958).

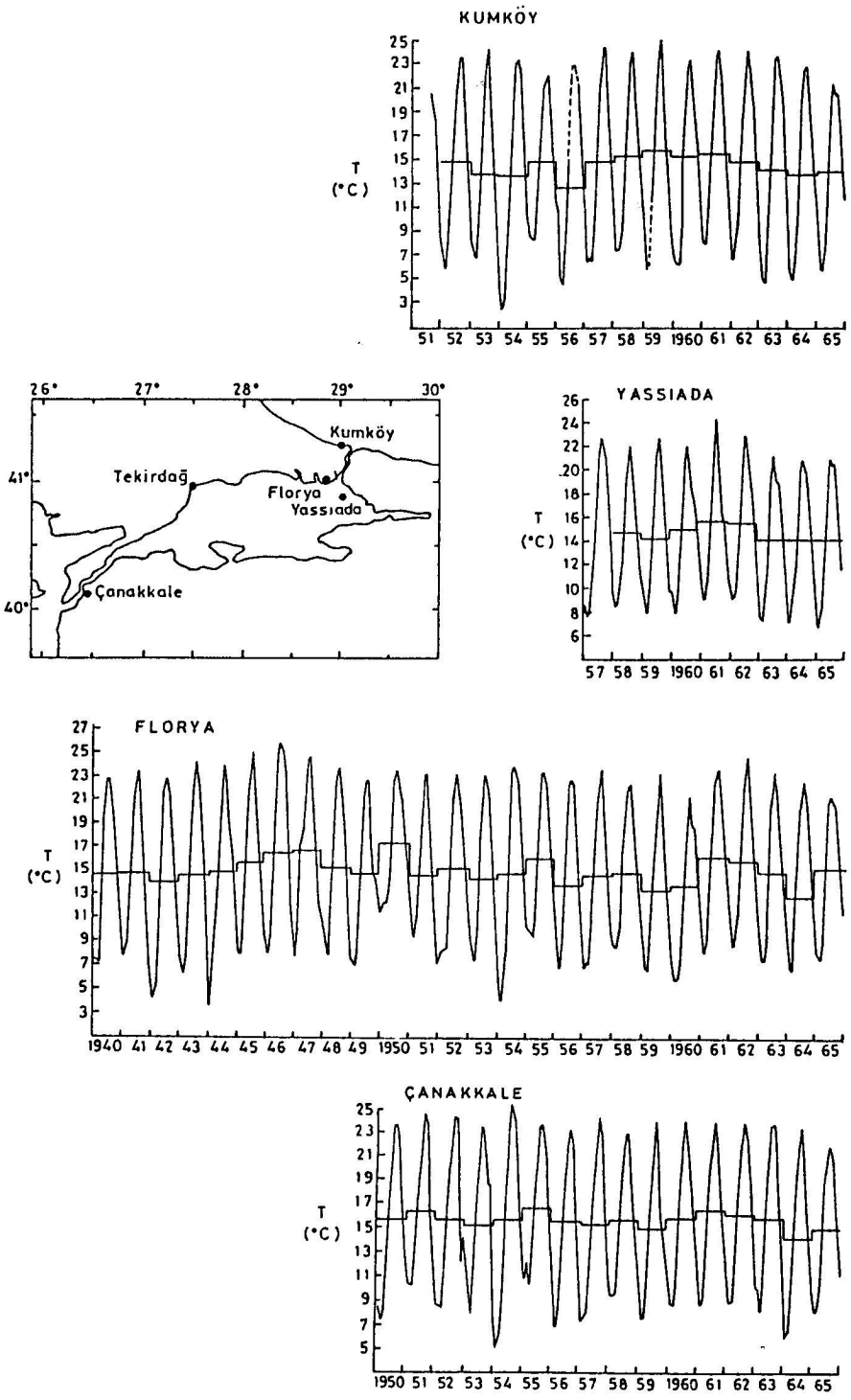


FIG. 11. Long term surface temperature measurements at various stations in the Marmara Sea.

The evidence also suggests that the mixing of the upper layer waters depend on the long-term variations in weather. For example, the upper layer salinity in the Marmara Sea attained a maximum of 30ppt during February 1987 as compared to the usual 25-27ppt observed during other winter periods. The near-surface (5m) salinity at all stations in the Marmara Sea (Fig.12) showed this exceptionally large increase of salinity relative to the winter months of other years. BAŞTÜRK, SAYDAM, SALİHOĞLU and YILMAZ (1990) showed that there was a concomittent increase in upper layer nutrients during the same year. The winter of 1987 was particularly severe and led to deep mixing events throughout the entire region, including an exceptional deep water formation event in the Rhodes Gyre region of the Eastern Mediterranean (GERTMAN, OVCHINNIKOV and POPOV, 1990) and a deepening of the main pycnocline in the Black Sea (H.I. SUR, personal communication). During the same period between May 1986 and July 1988, there was an extraordinary high productivity event detected from radioactive dating of fresh bottom sediments at the bottom of the Black Sea (MOORE and O'NEILL, 1991).

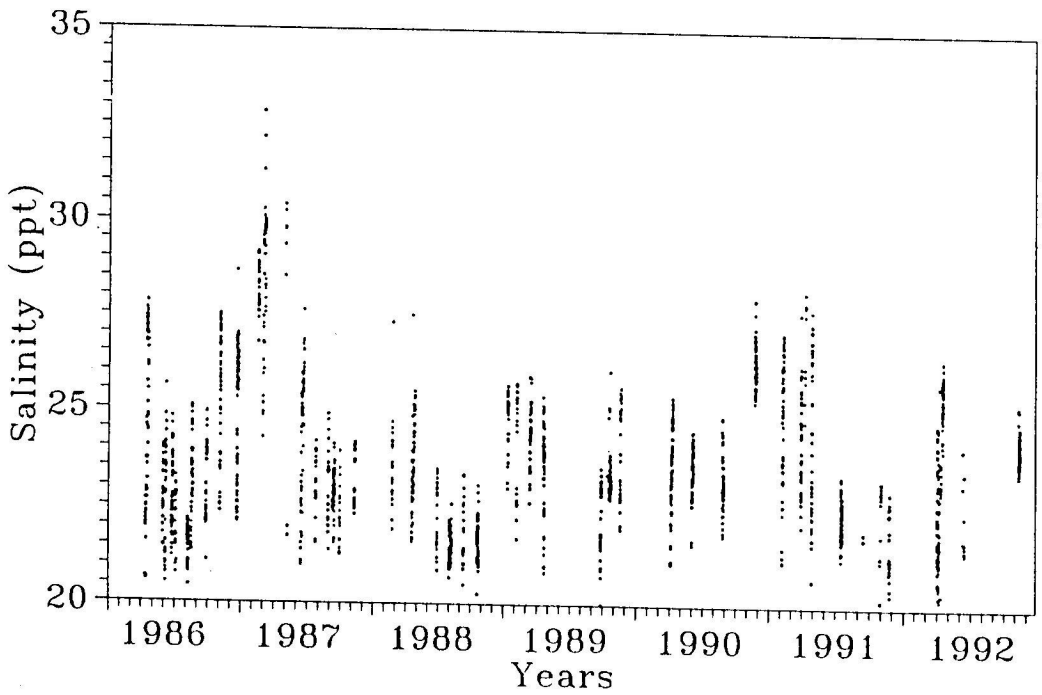


FIG.12. Surface salinity measurements (upper 10m average during the course of the measurements in the Marmara Sea. Each data point corresponds to a hydrographic station occupied in the basin.

5.4 Impacts on environmental health

Because the Sea of Marmara forms a transition between two larger seas of opposing character, it is influenced by environmental conditions in the adjoining waters. Pollution from terrestrial sources along its heavily populated shores and from its busy navigation lanes has caused a rapid deterioration of the marine environment. The Sea of Marmara is a migration route for fish species moving between the adjoining seas, and, in itself, is a region of high productivity. These adverse effects of recent decades have been seriously damaging.

Signs of eutrophication are becoming increasingly evident, especially in the shallow continental shelf regions, adjacent to the Bosphorus, and in semi-enclosed bay regions. It is unclear whether the process is being driven by nutrients coming from the Black Sea or from local sources. However, the eutrophication so evident in the adjoining Black Sea (MEE, 1992), is being driven by the increased nutrient supply from major rivers (a ten-fold increase since the 1950s in the case of the Danube river). These nutrients are in part exported into the Marmara Sea via the Bosphorus, amounting to 12,000 ton y^{-1} of total phosphorus, 190,000 ton y^{-1} of total nitrogen, and 1,520,000 ton y^{-1} of total organic carbon (POLAT and TUĞRUL, 1994). In winter, the nutrients which have remained unutilised in the colder waters of the Black Sea are delayed by several months in their transit through Marmara, which lead to substantial increases in spring-time productivity.

An almost equal amount of nutrients are entrained from below into the upper layer. The exit region of the Bosphorus is especially productive because the nutrients originating from the Black Sea combined with those entrained into the jet from below, give rise to a high recycling of nutrients (ÜNLÜATA and ÖZSOY, 1986; BAŞTÜRK, SAYDAM, SALİHOĞLU and YILMAZ, 1986, 1988, 1990).

6. UPPER LAYER CIRCULATION

6.1 Seasonal circulation

Two typical cases of summer circulation in the Marmara Sea, corresponding to the salinity distributions of Figs 9a,b are shown in Figs 13a,b. In May 1987 (Fig.13a) the coherent jet flow issuing from the Bosphorus initially flows to the south; upon reaching the coast of the Bozburun Peninsula, it is deflected west and then northwest, circulating around a closed anticyclonic circulation attached to the Thracian coast. Once the flow reaches the Thracian coast, it follows the coastline, bending once again southwestward off Tekirdağ, thence proceeding towards the Dardanelles Strait. This pattern of a meandering jet flow with wavelength matched to the length of the basin is the typical quasi-permanent pattern of the Marmara Sea circulation in the summer, as can be verified in Figs 5a,b. The size and shape of the S-shaped jet flow and the anticyclonic and cyclonic regions bordering it may be modified under particular circumstances. The dynamical balances leading to this pattern of circulation are unclear. However, in Figs 9a and 10, we note that the pool of low salinity waater in the eastern basin west of the jet, introduced there by the spring flooding of the Black Sea waters, could be partially responsible for driving the anticyclonic circulation and the bending of the jet, through horizontal pressure (density) gradients. Clearly, the basin geometry and the dynamics of the initial jet flow also determine the specific summer circulation pattern of the Marmara Sea under relatively weak wind forcing.

We note that the circulation pattern of Fig.13a matches very well with the upper layer salinity distribution shown in Fig.9a. This result was expected because it is the contribution of salinity rather than temperature which dominates the density distribution; the qualitative correspondence of salinity with streamfunction would be required, provided that the assumptions of geostrophy,

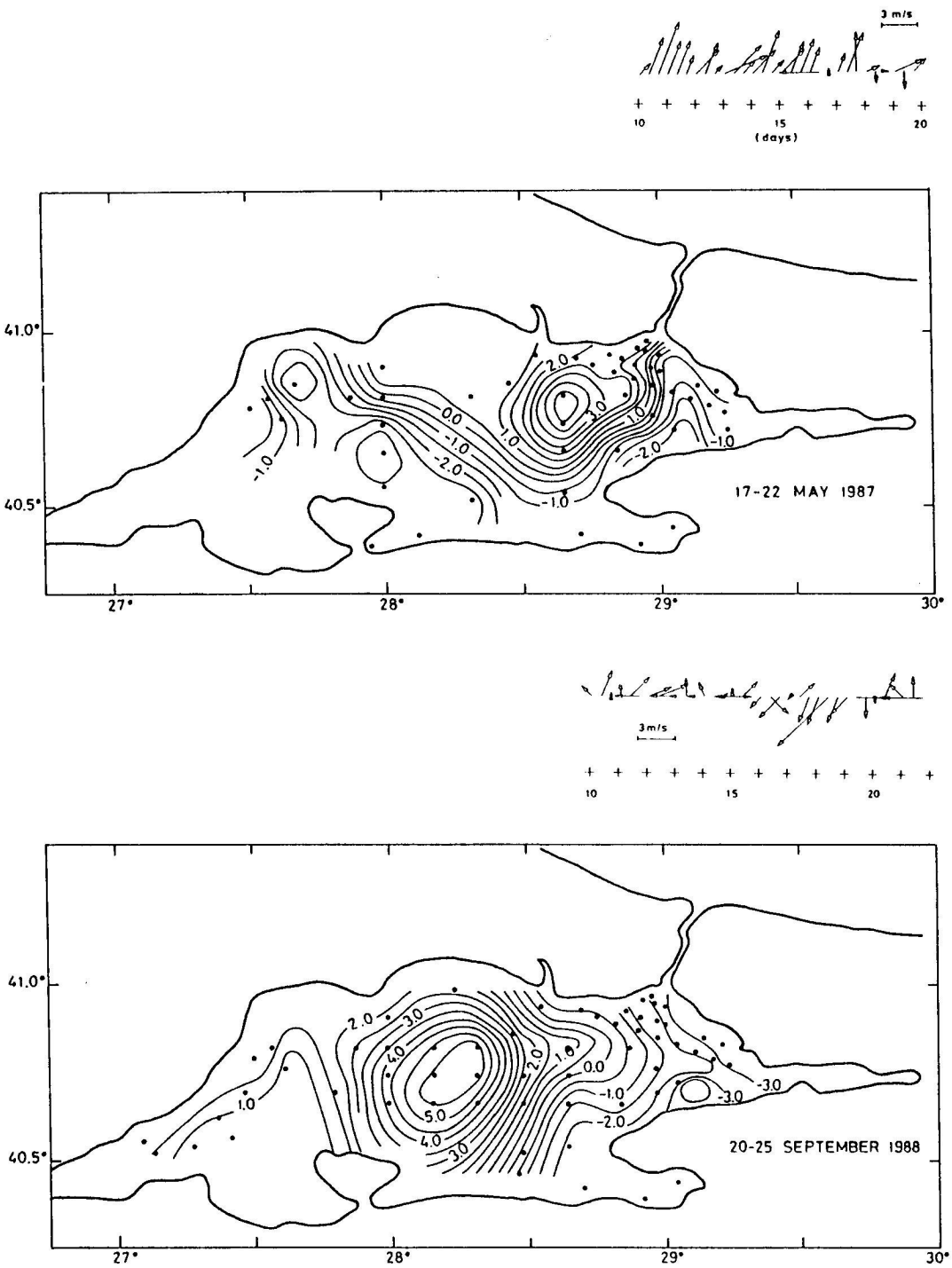


FIG. 13. Dynamic height anomalies distribution at 5m for (a) May 1987, (b) September 1988. The three times a day wind velocity vector stick plot, where north is up, is in the upper right corners measured at Florya.

in addition to the horizontally uniform halocline depth, the vertically uniform upper layer salinity and a motionless lower layer, would hold. Evidently, these assumptions were reasonably accurate in the case of May 1987. This classical pattern of circulation was observed in a number of other cases during summer months.

The upper layer jet flow exiting from the Bosphorus is less clearly defined in the example of September 1988 (Fig.13b), when the anticyclonic circulation occupying a greater part of the Marmara Basin was stronger than in May 1987. We conclude that the clockwise circulation continued to develop in summer, in response to the increased and uninterrupted flow of Black Sea waters through the system. Although the Bosphorus inflow tends to decrease significantly during autumn, the circulation which has developed persists until it is destroyed by predominantly wind-driven motions in the late autumn and winter. In both the examples shown in Figs 8a and b, the region was under the influence of mild winds (as shown by the insets showing the variations in wind velocity at Florya).

The prevailing inflow conditions of the Bosphorus jet are illustrated by the distribution of current velocities measured by ADCP in the near surface (10m) of the Bosphorus-Marmara junction region, during the periods of maximum and minimum Black Sea annual discharge during June and October respectively (Figs 14a,b). In June 1991, the jet is coherent and directed towards the south (Fig.14a). Recirculations appear on both sides of the jet in the near field. In October 1990 (Fig.14b) the ADCP velocity measurements at 17m coincide with the circulation inferred from salinity distribution, showing a cyclonic eddy in the eastern Marmara region. Because the Bosphorus discharge has evidently decreased during this season there is no sign of a jet. The cyclonic circulation appears to have been generated by buoyancy introduced from the Bosphorus inflow.

Another case of autumn circulation which differs significantly from the typical summer circulation is shown in Fig.15. In fact, the sense of the circulation is reversed in many areas of the Marmara Sea. There is a cyclonic circulation in the eastern basin, an anticyclonic circulation in the central basin, and northeasterly flows along the northern region. Even the flow through the Dardanelles has reversed, with the upper layer waters flowing into the Marmara Sea from the Aegean. This situation is likely to be a result of an almost purely wind-driven circulation under the conditions of decreased throughflow. Nor is there any indication of the Bosphorus jet, as during October 1990 (see above). Although we do not have continuous wind data for this case, the winds recorded on board ship were from the southwest with speeds of 10-15ms^{-1}. The reversal of the normal upper layer currents in alignment with the winds suggests a very rapid response to wind forcing. Because the upper layer thickness of the Sea of Marmara is only 25m and the basin is relatively small, one would expect adjustment to wind within a short inertial period (days).

Finally, a circulation pattern for the early spring is shown in Fig.16, with the ADCP velocity measurements superimposed together with the dynamic height anomaly. In March 1992, although the Bosphorus jet with high velocities was clearly identified, and similar rapid flows were observed near the Dardanelles on the western side, the circulation exhibits much the same small scale eddies and the breakdown of the jet flow that were observed earlier during the summer. The wind velocity (inset) indicates variable forcing during March 1992, with strong northeasterlies during the cruise period. The typical wind speeds of 5ms^{-1} indicated by the measurements at the land station were actually about half those measured on board. The northerly winds would be expected to have a reinforcing effect on the net flow of Black Sea waters through the system. Indeed, the Bosphorus upper layer flux during the same period was on the order of 20000m^{3}s^{-1} (LATIF, ÖZSOY, BEŞIKTEPE, OĞUZ and SUR, 1992a), and this increased net flow is evident from the large currents observed near the junctions with the Straits. However, despite the increased net throughflow, a coherent jet-like flow similar to that observed in the summer does not seem to be maintained, and the circulation tends to disintegrate as a result of the wind forcing.

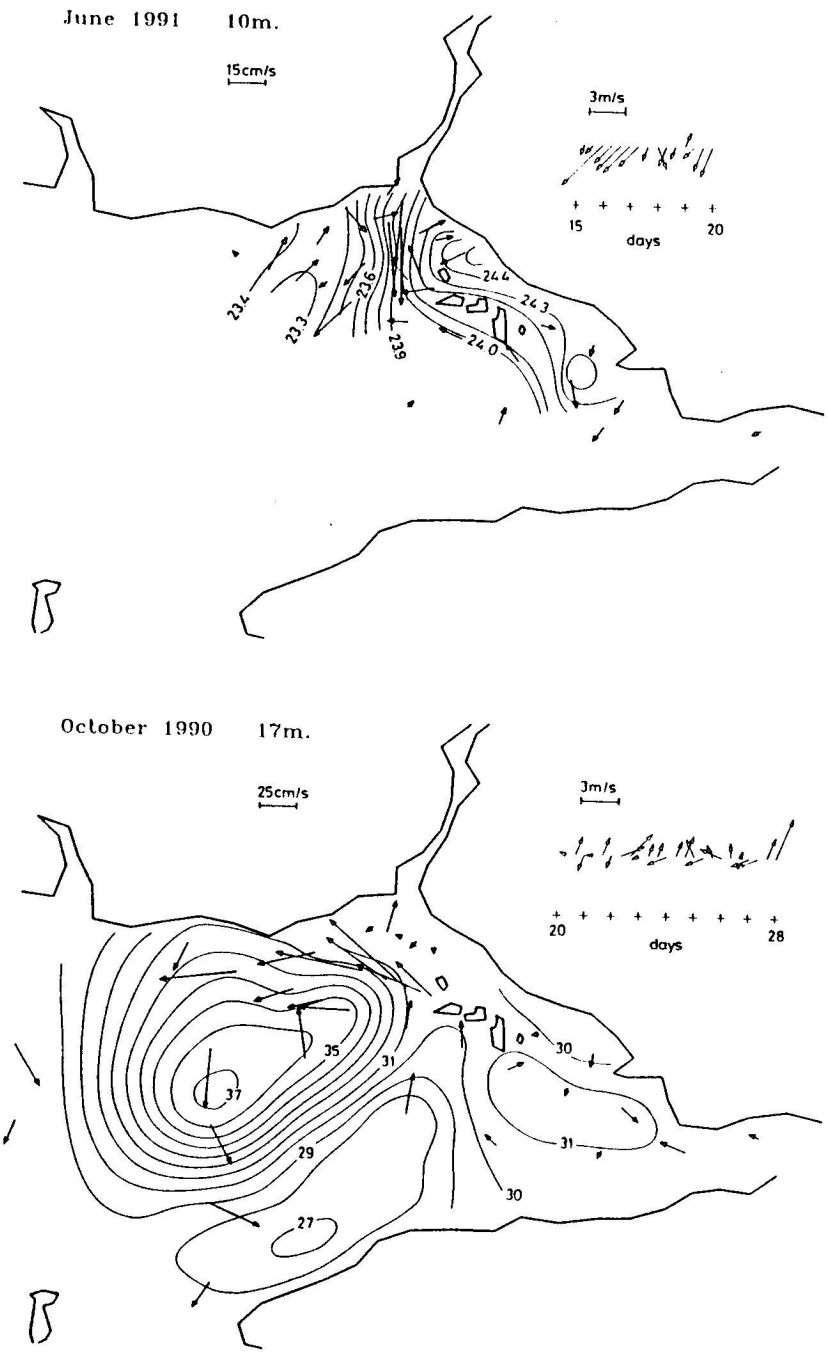


FIG. 14. ADCP measured currents in the vicinity of the Bosphorus strait (a) June 1991 (at 10m), (b) October 1990 (at 17m) superimposed on the salinity distribution at the same depth. The wind velocity vector stick plots, where north is up, are in the upper side of the figures measured at Florya.

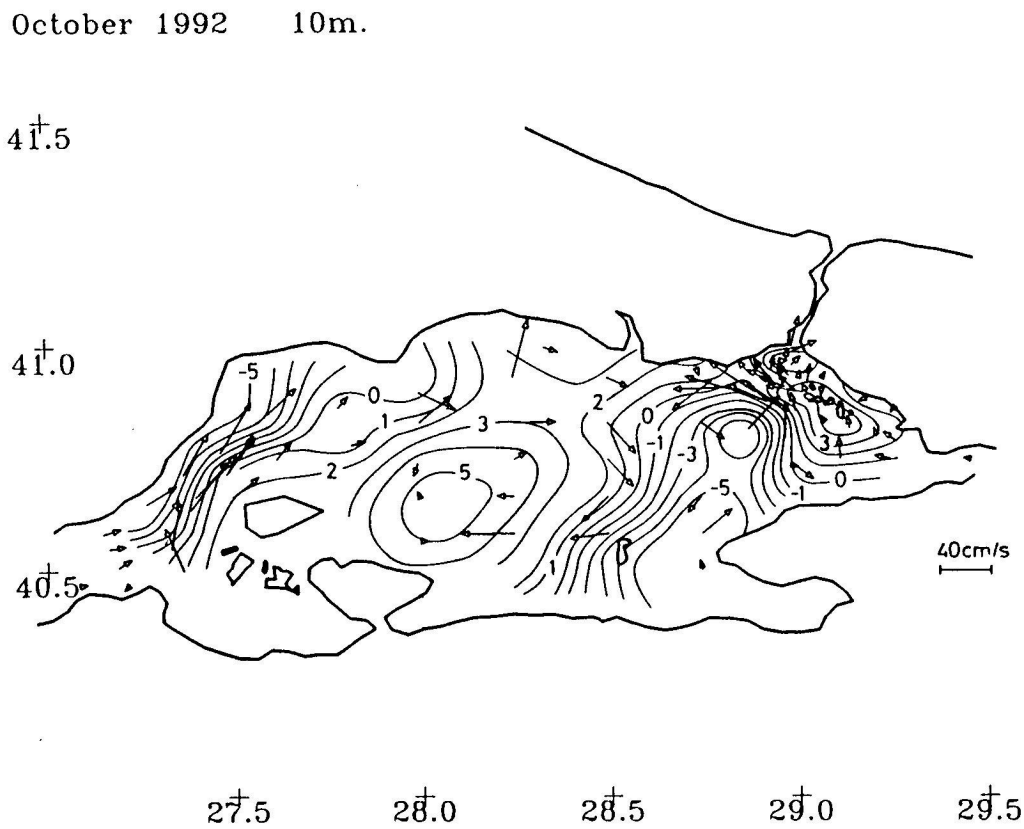


FIG. 15. ADCP measured currents at 10m superimposed on the DHA during October 1992.

The small scale circulations generated in the autumn-spring period are consistent with the Rossby internal radius of deformation (PEDLOSKY, 1987), $L_D = g'H/f$, where g' is the reduced gravity, H is the depth of the upper layer, and f is the Coriolis parameter. Using typical values of $f = 10^{-4}$, $g' = 0.1 m^2 s^{-1}$, and D = 25m, L_D is found to be about 17km, comparable with the scales of the eddies formed.

6.2 The Bosphorus Jet

The surface outflow issuing from the Bosphorus into the Marmara is illustrated in Fig.16 for March 1992. We provide some details of its distribution in terms of density (σ_t) and velocity sections across the axis of the Bosphorus in Figs 18 and 19 for stations shown in Fig.17. The velocities in Figs 18 and 19 were mapped while the ship was moving between stations. The upper layer properties are variable as a result of the presence of the buoyant jet, which at the time extended from Station S5 to M17. The jet is identified by the outcropping of density isolines at Stations S5 and M17 in Figs 18a and 19a. The Bosphorus outflow velocities were southerly near the exit region (at S5) but were south-easterly at offshore section (Fig.19). The horizontal gradient of density across the jet with increasing currents near the surface is consistent with geostrophy (the thermal wind relation). The trapping of light fluid in the anticyclonic region west of the jet, and its consistency with the jet bending have been touched upon earlier with regard to the summer circulation. At stations S5 and M17 the core of the Bosphorus outflow jet with the highest velocities was not exactly alligned, indicating there was some meandering, and possibly transience, associated with the turbulent jet structure.

7. HYDROGRAPHIC VARIABILITY OF THE SUBHALOCLINE WATER MASSES

7.1 Water masses

The θ-S diagrams of two stations from the western and eastern parts of the Marmara Sea from one cruise are shown in Fig.20 to illustrate lower layer (sub-halocline) water mass structure. Station K50J34, located at the deepest part of the western basin, is directly influenced by the Dardanelles inflow. The other station, K46L00, is in the eastern basin and away from direct influence of the Dardanelles inflow. The upper part of the halocline, which includes Black Sea waters, is not shown, and expanded scales are used in order to emphasize sub-halocline water characteristics and variability. The θ-S diagrams show a negative trend for temperature and salinity below a depth of 100m (excluding the salinity maximum occurring at intermediate depths). Four different water masses can be identified at K50J34: a layer with maximum values of temperature and salinity is located below the halocline and is limited to the upper 150m; an intermediate salinity minimum occurs at depths of about 300m; below which is a cold layer with a maximum salinity between depths of 650-800m, and finally there is bottom water with a minimum temperature and low salinity. Although the first three of these water masses occur in the eastern part, the bottom water layer with minimum temperature and salinity is absent in the eastern basin. As a result of the sill separating the basins, the bottom density of the eastern basin is lower than that in the western basin.

7.2 Renewals of the subhalocline waters

The subhalocline waters of the Marmara Sea are supplied by the inflow of Mediterranean water through the lower layer of the Dardannelles Strait. The seasonal rnewal of the bottom waters was recognized after measurements of relatively high oxygen concentrations near the bottom especially

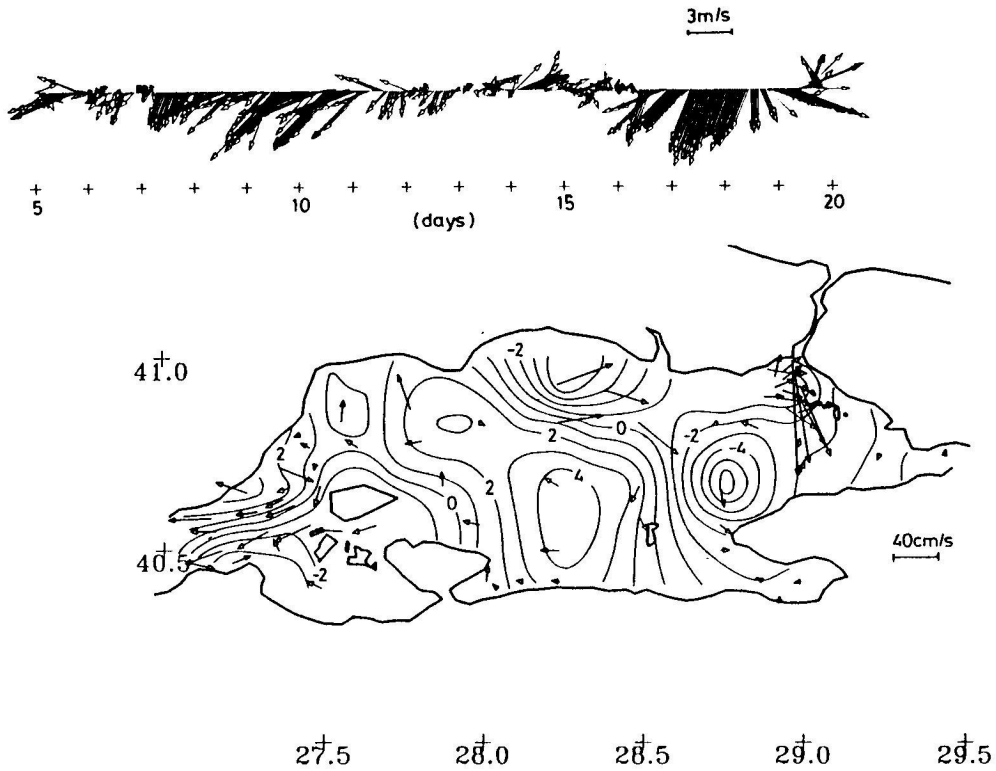


FIG. 16. ADCP measured currents at 10m superimposed on the DHA during March 1992. Hourly wind velocities, where north is up, measured at Florya is in the upper side of the figure.

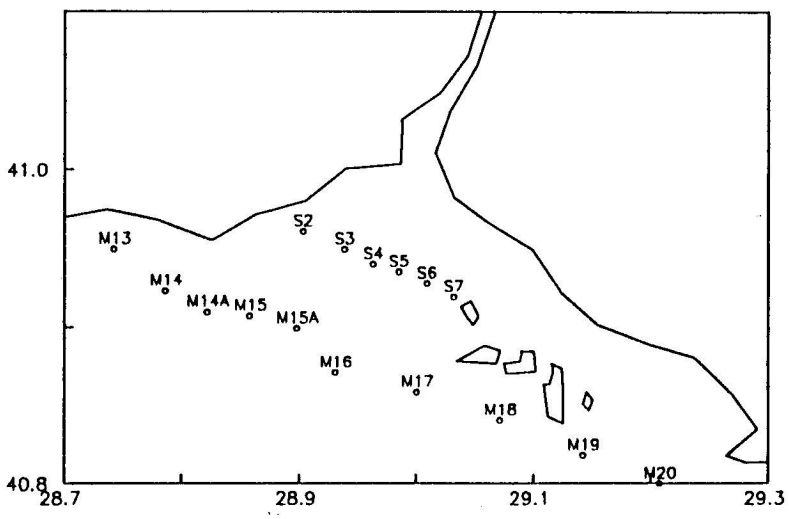


FIG. 17. Oceanographic stations visited in the vicinity of the Bosphorus strait.

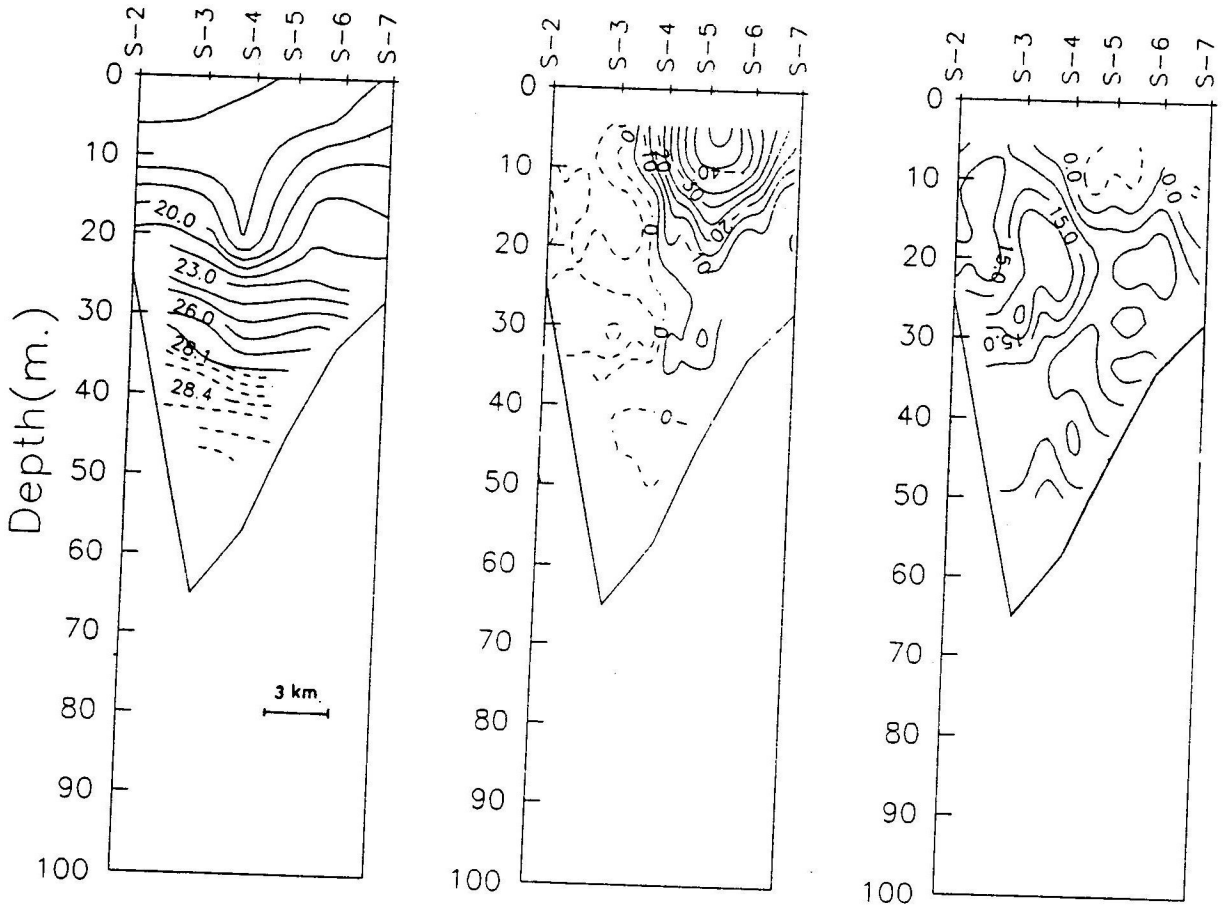


FIG. 18. Vertical sections across the main axis of the Bosphorus for 6 March 1992; (a) sigma-theta; (b) northerly (positive) velocities (dashed lines); (c) easterly (positive) velocities (dashed lines). Positions of the stations shown in Fig.17.

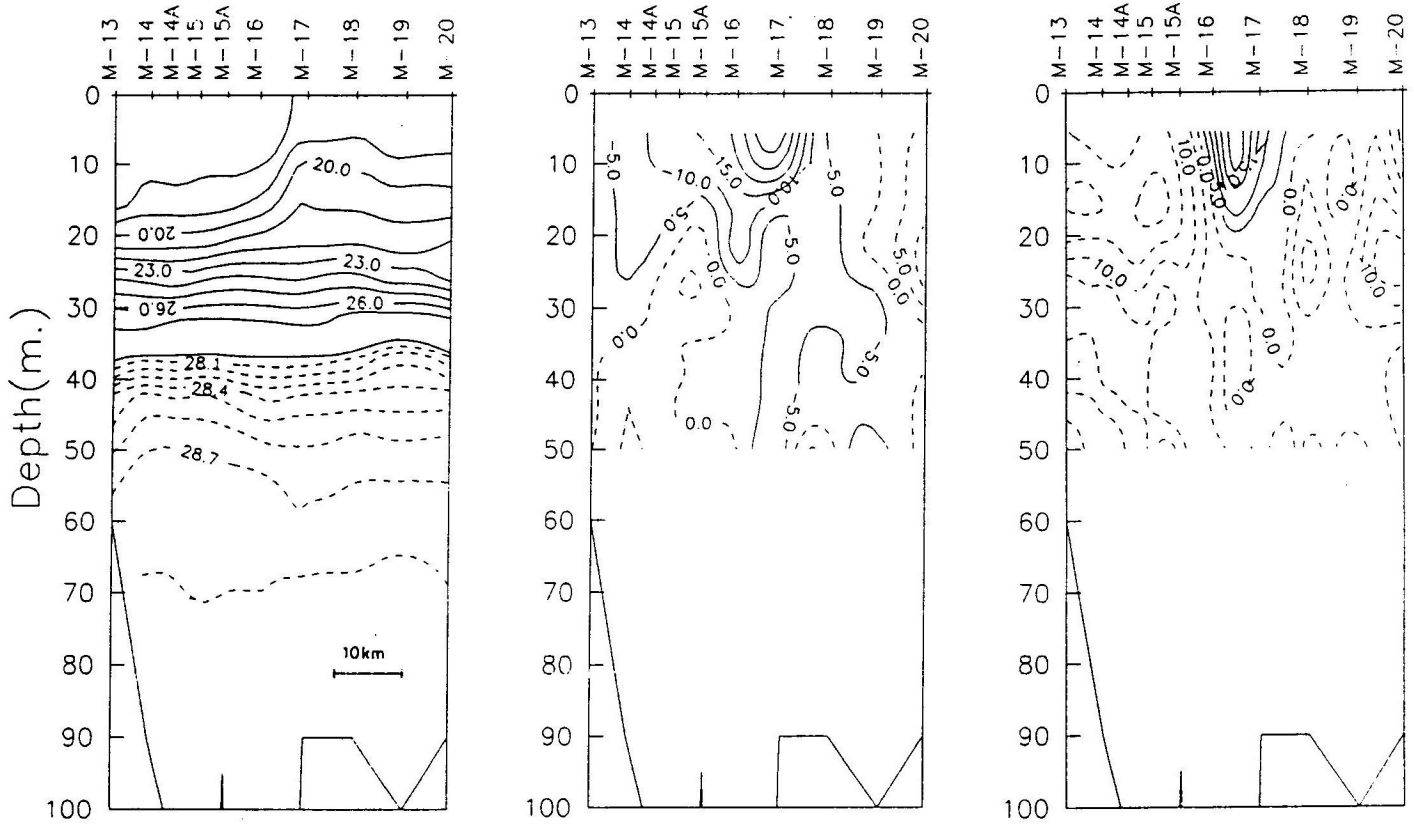


FIG. 19. As for Fig. 18 but for offshore stations.

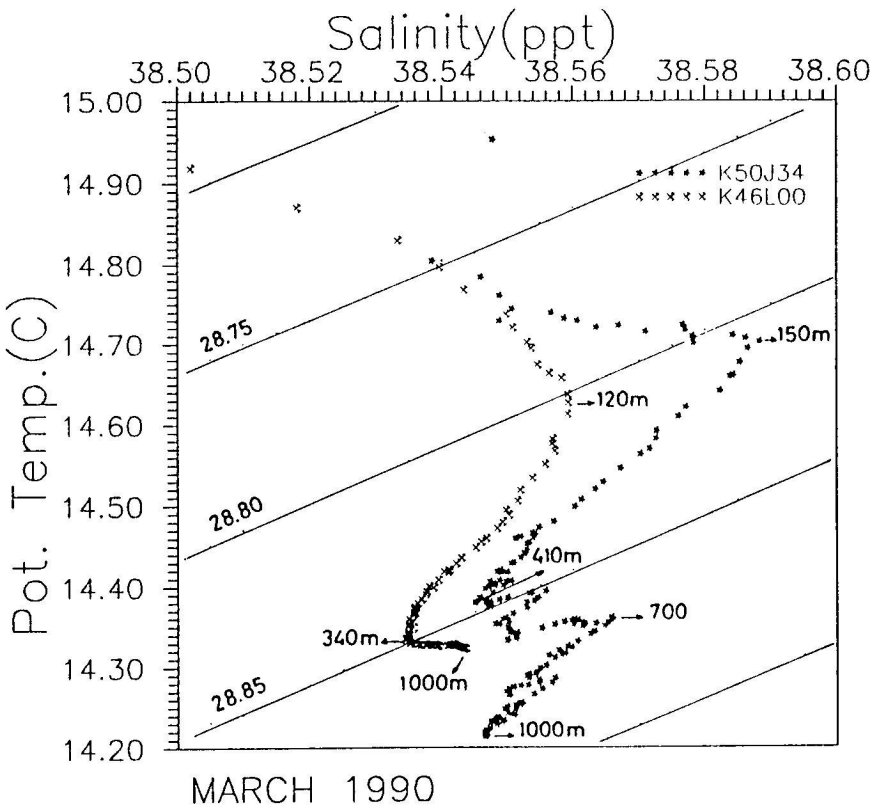


FIG.20. The θ-S diagrams from two selected stations in the eastern and western parts of the Marmara Sea in March 1990.

in the western basin. The spreading into the interior of the influence of the waters intruding from the Aegean Sea and the resulting renewal mechanisms are complex processes which have been identified recently by ÖZSOY, OĞUZ, LATIF and ÜNLÜATA, (1986), ÜNLÜATA and ÖZSOY (1986) and BEŞİKTEPE (1991). A simplified 'filling box' model of the renewal mechanism ignoring horizontal variations within the interior has been constructed by BEŞİKTEPE, ÖZSOY and ÜNLÜATA (1993).

The Sea of Marmara is comprised of three deep basins separated by sills, so the spreading of the deep waters is determined essentially by bottom topography. The most striking direct evidence for renewal is provided by the temperature distributions. There is a clear difference in the temperature profile of the eastern basin and the other two, which was first recognised by NIELSEN (1912) based on just three casts in the Sea of Marmara. The same difference was reported

independently by ÖZSOY, OĞUZ, LATIF and ÜNLÜATA, (1986), without knowledge of Nielsen's earlier results. In the western and central deep basins (Fig.21), the temperature profiles despite some fine structure evidently resulting from the mixing of the Dardanelles intruşion, are approximately isothermal below 300m, indicating efficient vertical mixing, and consequently the potential temperature decreases monotonously with depth. In contrast, the deep waters of the eastern basin are approximately isentropic, with a uniform distribution of potential temperature, and a monotonous increase of temperature with depth resulting from adiabatic compression. The nearly isentropic conditions below a depth of 200m in the eastern basin indicate that both vertical mixing and exchanges with the western basin are negligible. This difference in the temperature between adjacent basins results from the geometry of the sills separating them. The sill connecting the western and central basins is relatively shorter and deeper than the long narrow sill separating the central and western basins. Consequently, the effects of the deep water renewals occurring in the western and central basins do not penetrate into the eastern basin.

7.2.1. Seasonal variability. The properties of the sub-halocline waters displayed earlier in Fig.20 are relatively constant, with potential temperature of 14.5°C, salinity of 38.5, σ_θ of 28.6, and oxygen concentration of 2ml l^{-1}. In the subhalocline waters, the oxygen saturation ratio is 0.2, as a result of the balance between consumption and influx. However, relatively small changes occur in the properties in response to the intrusions from the Dardanelles.

In order to specify the temporal and spatial variability of the subhalocline waters, we have analyzed the temperature and salinity transects along the main axis of the Marmara Sea for four different months, each representing different seasons (Figs 22-25). The inflowing dense water sinks to its equilibrium depth after entering from the strait (BEŞİKTEPE, ÖZSOY and ÜNLÜATA, 1993). The sinking of the plume shows well defined seasonal variations as a result of the seasonal variations in the incoming water. During the winter months the Dardanelles plume is a cold dense water which sinks to the bottom. This dense water mass flows into the westernmost basin, where it accumulates and displaces the 'old' water upwards. The 'old' interior water upwells to balance the sinking plume, with an upward velocity which has to balance the input of the plume, to maintain continuity. This upward velocity results in an upward tilting of the isopycnals which was observed every late-spring, and a flow of bottom water from west to east (BEŞİKTEPE, ÖZSOY and ÜNLÜATA, 1993).

In summer, during July 1988 (Fig.22), the incoming Dardanelles flow was seen as a thin layer of warm and saline water near the bottom (~100m) over the shelf which, however, did not produce a significant density anomaly. Therefore, at that time the maximum depth to which the Dardanelles inflow influenced the interior of the basin was 100-200m and it was flowing eastwards through the upper part of the lower layer, where it was feeding the salinity maximum located around 100m. The relatively smooth distribution of temperature and salinity at depths >400m still showed residual signs of an earlier deep water intrusion, in the region of higher salinity below 400m (Fig.22b). The core of this intrusion was still relatively colder (T=14.2°C) than its surroundings, as was characteristic of intrusions earlier than July 1988. This water mass filled the first basin completely and lifted the western water column. However, the sill between the western and central depression restricted the flow.

In autumn, during September 1988 (Fig.23), the inflowing water over the shelf region was warmer and more saline than the interior water and of similar density. So the inflowing intrusion was neutrally buoyant and flowed across the Marmara Sea immediately below the halocline. In the deeper parts of the Western Basin, a water mass was tilted up towards the east enough for it to flow over the sill between the western and central basins. As this water mass diffused eastward it formed persistent deep fronts. At this time, the central basin had not yet been filled with the new intrusion, and the bottom water was still less salty than that found between 400-800m.

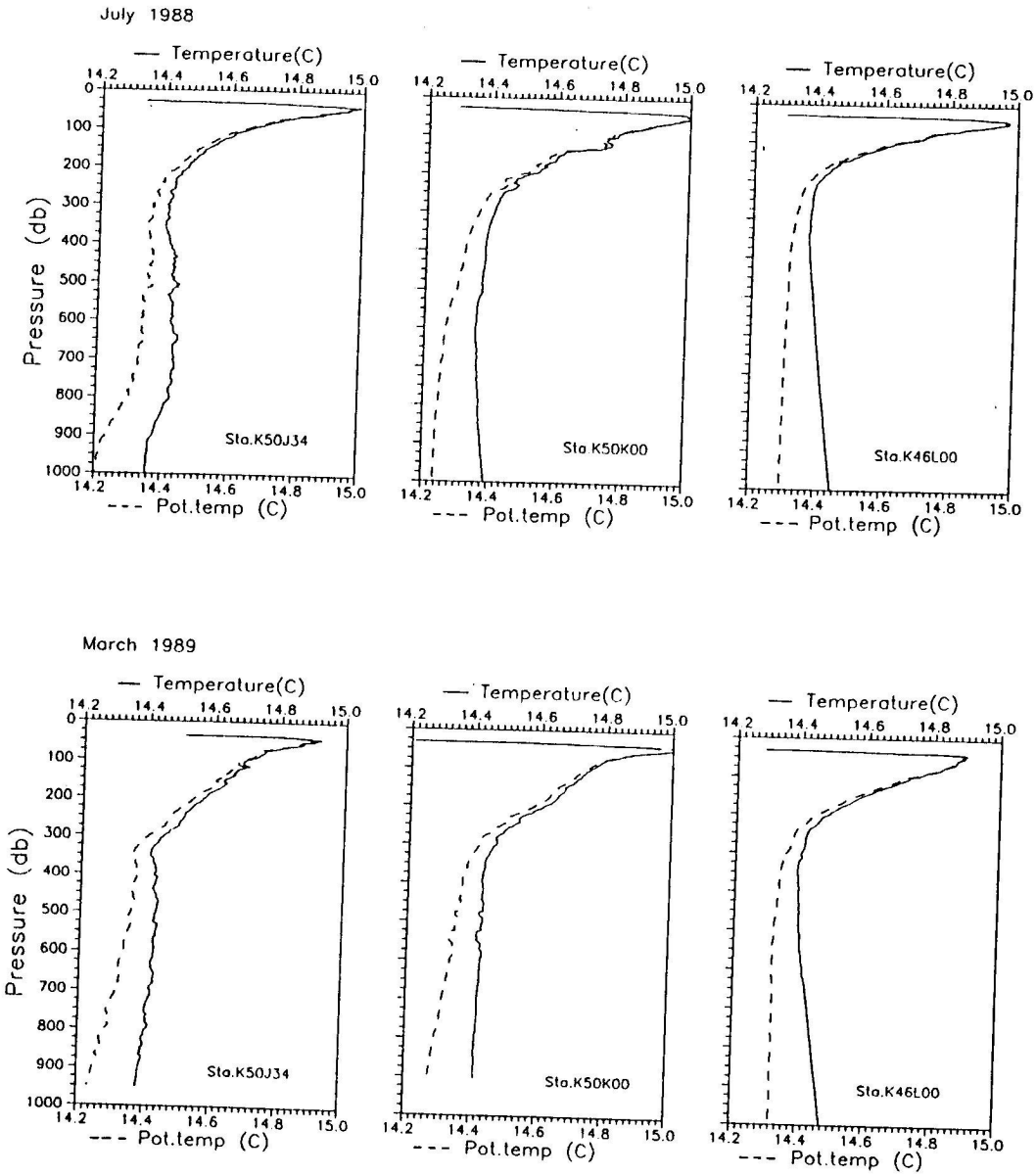


FIG.21. Deep water enlarged scale profiles of temperature and potential temperature in the three deep basins of the Marmara Sea in (a) July 1988; (b) March 1989.

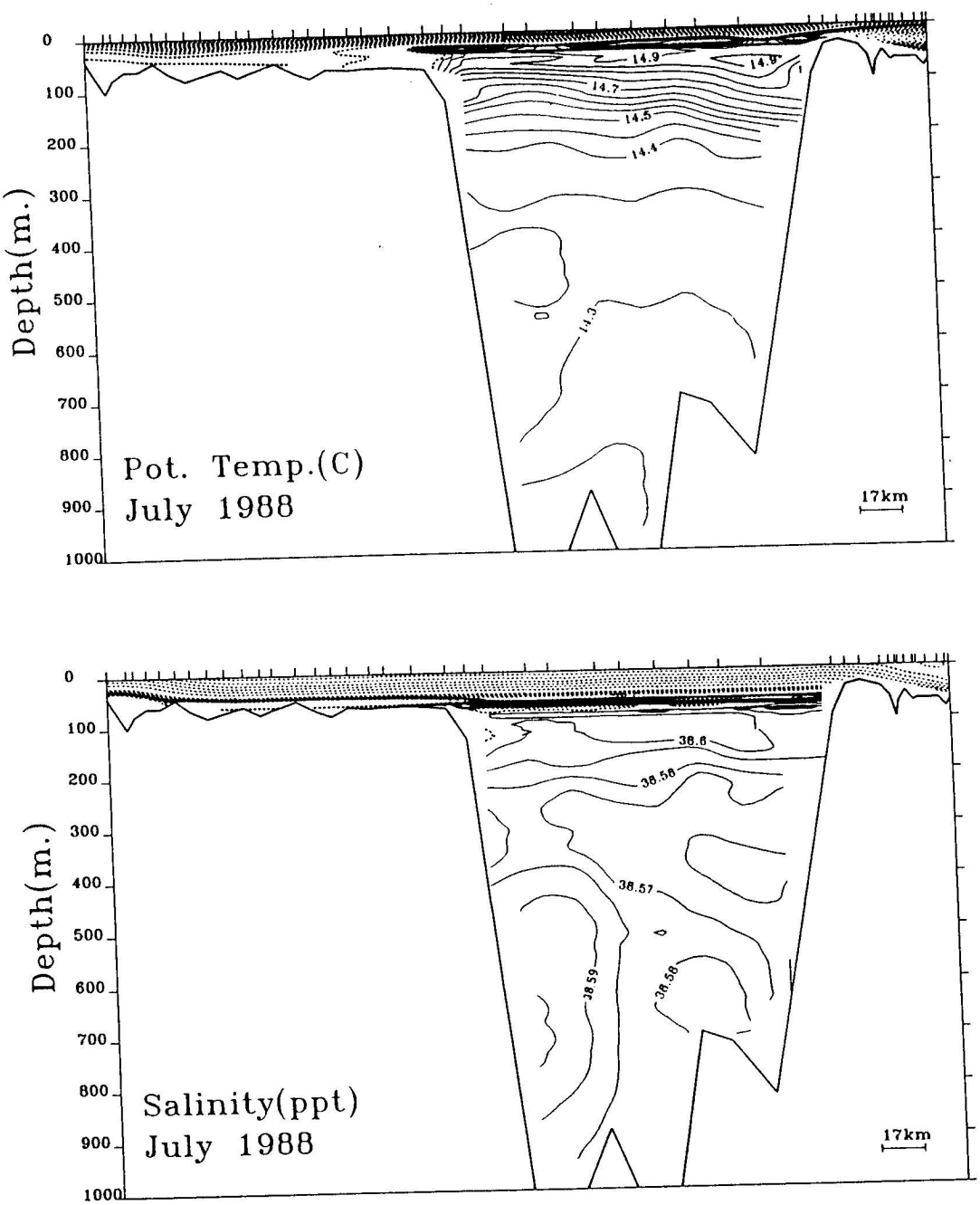


FIG.22. (a) Potential temperature; (b) salinity transects from the Aegean Sea to the Black Sea along the main axis of the Marmara Sea, July 1988.

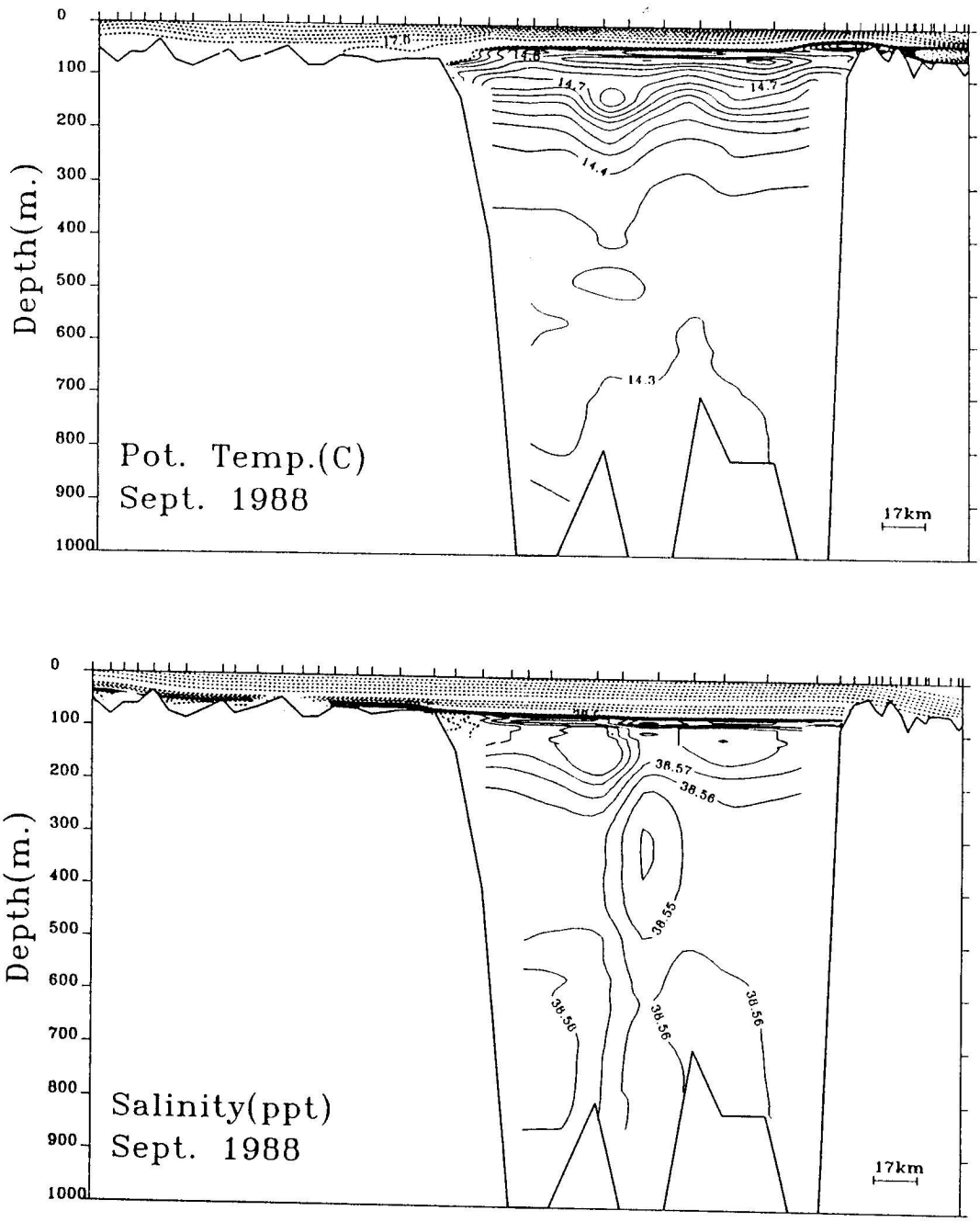


FIG.23. As in Fig.12, but for September 1988.

The shallowness of the intrusion of the Dardanelles inflow during the summer - autumn of 1988 (Figs 22-23) is typical for these seasons and indicates that the inflowing water does not always sink to the bottom of the basin. When the inflowing water has insufficient negative buoyancy, it traverses the Marmara Sea through the upper part of the subhalocline region, which may explain the presence of temperature and salinity maxima (of 15°C and 38.6ppt) below the interface. So the layer including these maxima could be formed by an average influence (in the climatological sense) of the shallow summer/autumn intrusions of Dardanelles water.

In December 1988 (Fig.24), the waters intruding into the shelf region were continuing to exhibit warm and saline anomalies which were only slightly denser than the waters in the interior at the same depth. The maximum depth of penetration was, therefore, about 300m, marked by the lower boundary to a series of salinity and temperature anomalies. Because there is entrainment from both above and below, the incoming water enters as a stratified plume, and since, in such stratified plumes the less dense upper part will reach its equilibrium depth before the lower more dense parts (AAGARD, SWIFT and CARMACK, 1985), the plume interleaved at different depths. In December 1988, beyond the shelf break of the Dardanelles, thermohaline fronts marked two intruding anomalies at depths of 75-125m and 225-250m. The horizontal extent of these interleaving layers was about 20km. The flow of the bottom waters over the sill from west to east continued to fill the central depression with high salinity water. The deep thermohaline fronts previously seen in September 1988 had disappeared and the salinity minimum was less clearly defined. The flow was insufficient to surmount the sill between the central and eastern basins.

By early winter (Fig.24) the depth of penetration had increased as a result of the increased density of the inflowing water, and a further increase in density by the end of winter allowed the plume to sink to the bottom of the western basin (Fig.25). Cold, dense waters entered with the lower layer flow through the Dardanelles and consequently anomalous waters were seen on the western slope of the western basin. It is often difficult to follow such anomalous water along the entire length of the plume-like flow, because of the difficulty of sampling close to the steep slopes. Also a detailed inspection of the available data shows that the trajectory of the descending waters follows a three-dimensional path along the southern slopes of the western basin before finally arriving at the bottom. However, the sinking of the plume did not produce significant temperature and salinity anomalies in the deeper parts of the basin, perhaps because the inflow from the Dardanelles was reduced. Bottom water penetrating the eastern part of the Marmara Sea from the west had salinities >38.55ppt.

7.2.2. Interannual variability. The examples given above show that both the depth of penetration and the degree of modification of the interior water by the sinking plume depend strongly not only on the ambient stratification in the interior of the Sea of Marmara, but also on the seasonally changing temperature and salinity (density) characteristics of the adjacent waters of the Aegean Sea, which, in turn, are a function of the meteorological conditions and the circulation characterizing the neighbouring sea.

Although the general characteristics of the sinking plume and the subsequent renewal of the interior have well defined seasonality, interannual variabilities also occur. These interannual variabilities, the modification observed in the sub-halocline water mass, are illustrated by the variations of the temperature (upper panel) and salinity (lower panel) profiles at Station K50J34, a deep station close to the Dardanelles inflow in Fig.26. At the beginning of summer, the temperature and salinity of the water mass between 300-600m are higher than those of the surrounding water. This layer is modified by internal mixing duing the autumn, to become similar in character to the surrounding waters.

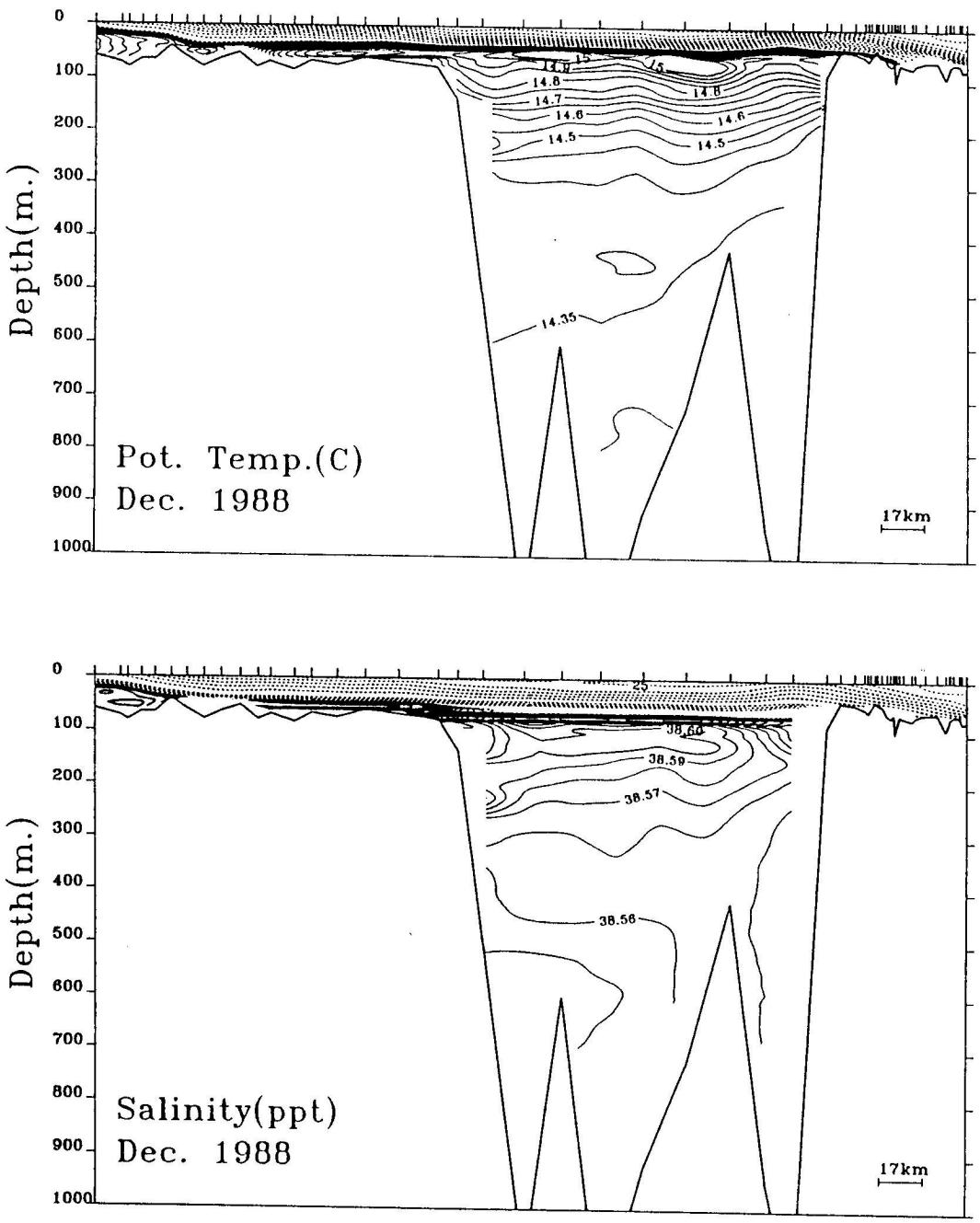


FIG.24. As in Fig.12, but for December 1988.

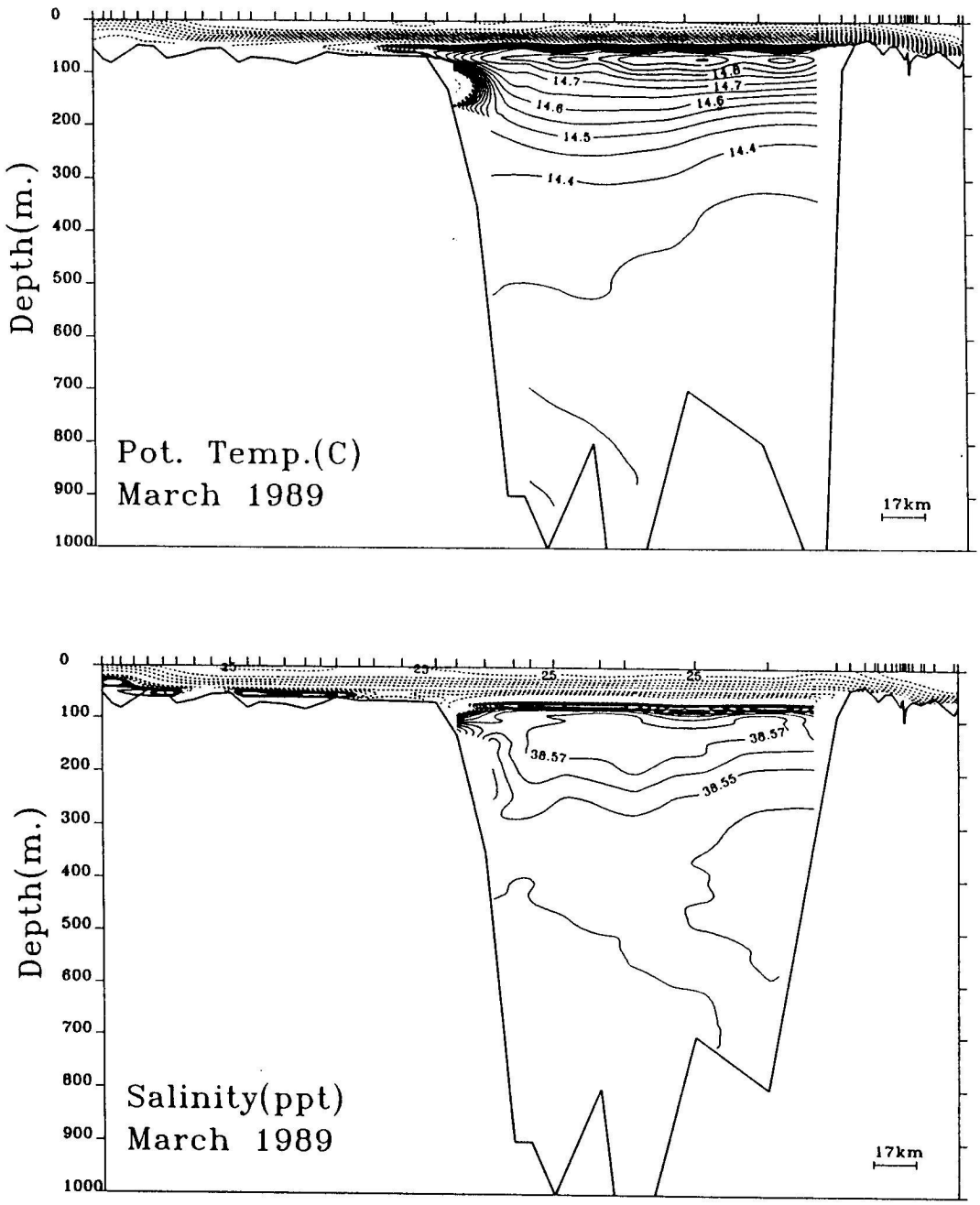


FIG.25. As in Fig.12, but for March 1989.

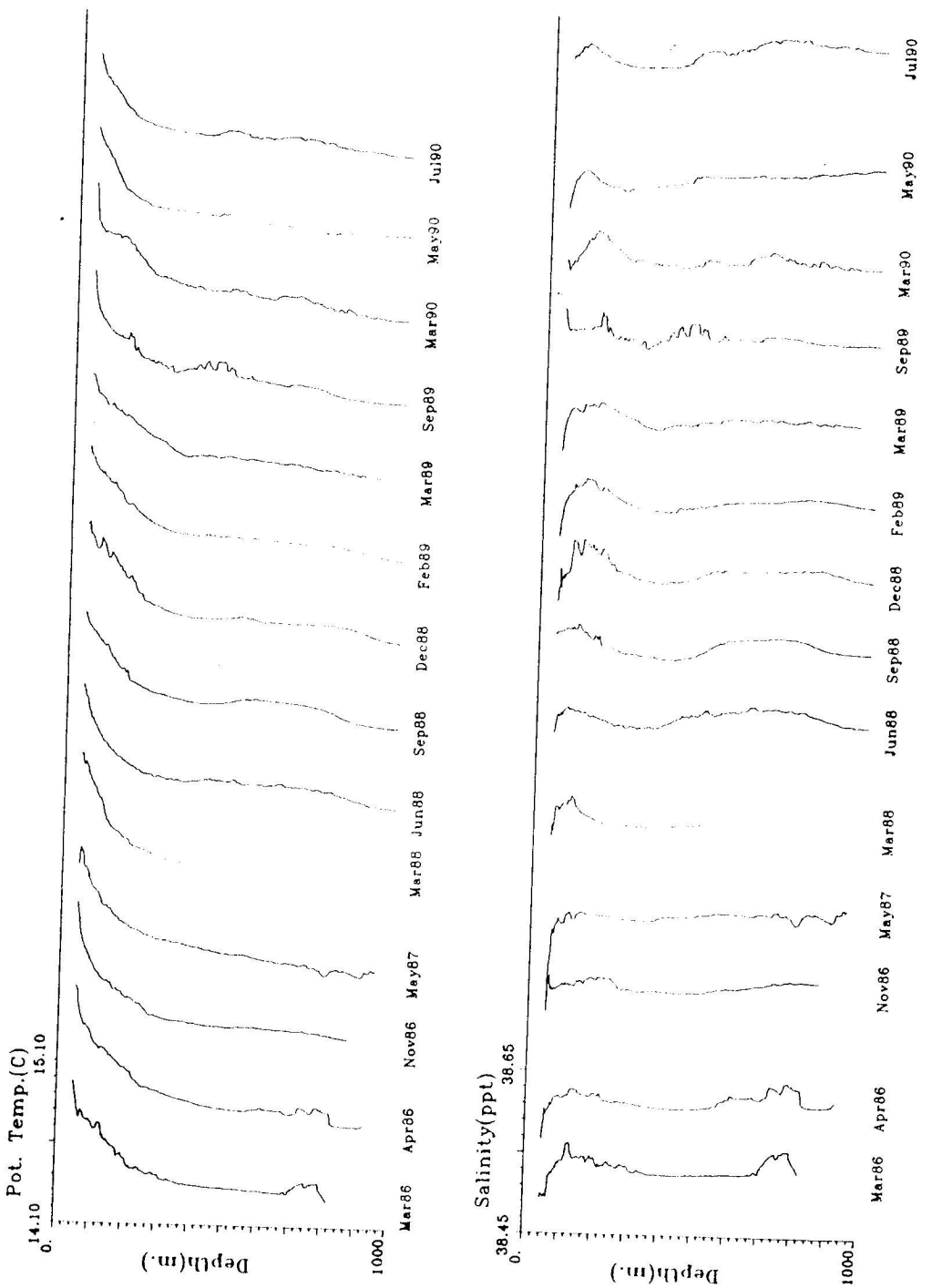


FIG.26 (a) Potential temperature; (b) salinity profiles taken at Station KS0034 from March 1986 to July 1990.

The temperature and salinity maxima in the upper part of the profiles persist throughout the year, but are intensified during autumn. The dense waters penetrating into the deeper part of the basin were either warmer and more saline (e.g. March 1986) or cooler and less saline (e.g. May 1987) compared to the interior, depending on the seasonal properties in the Aegean. As a result of intrusions of varying densities, interleaving is observed at various depths in the profiles throughout the year. An increase in the salinities between 500-800m is seen in July 1988. Subsequently, the anomaly disappears as a result of internal mixing and a series of fine structures were observed in summer 1989. The anomalies reappeared in July 1990, as a result of new intrusions.

The coldest Dardanelles inflow was observed in the winter of 1987, and although we did not collect data in the Marmara Sea during that winter, during the subsequent cruises in May 1987 we observed the most thorough deep water renewal of our observations.

7.2.3. Ventilation. Below the halocline the water is permanently deficient of oxygen despite the supply of oxygen-rich water through the Dardanelles Strait (Fig.27). The saturation ratio of the sub-halocline waters is of the order of 0.1-0.3. This is primarily a result of natural processes, and, like the anoxic conditions in the neighbouring Black Sea (STANLEY and BLANPIED, 1980), appears to have existed for historical periods (ÜNLÜATA and ÖZSOY, 1986). The continuous supply of oxygen prevents the development of anoxic conditions, but can not totally compensate for the oxygen demand created by the vertical flux of particulate organic matter (POM) originating from the upper layer.

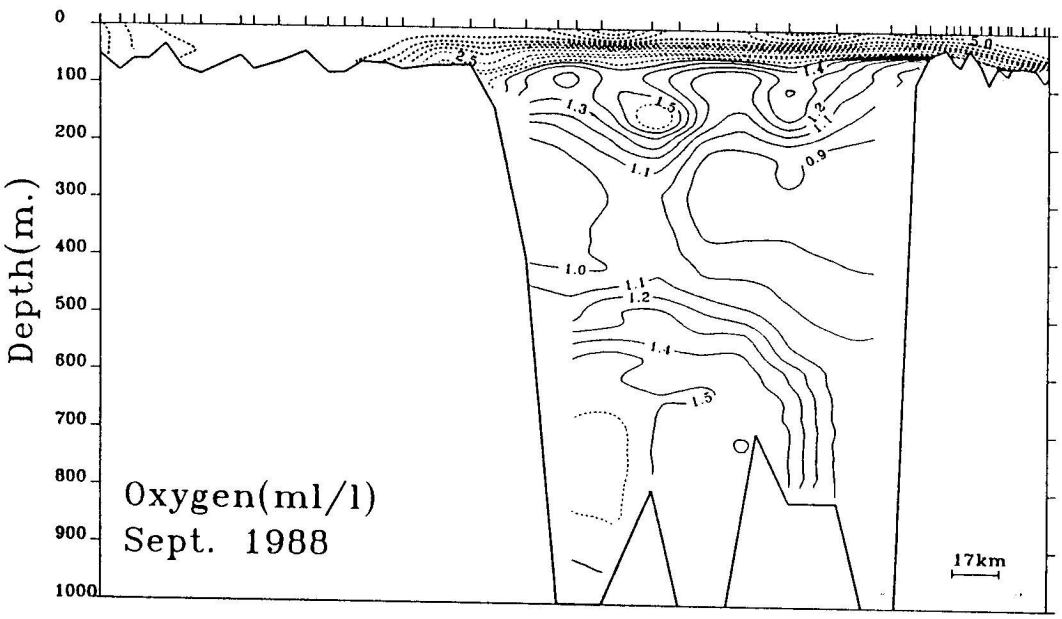


FIG.27. Oxygen transect from the Aegean Sea to the Black Sea along the main axis of the Marmara Sea, September 1988.

The sub-halocline distribution of dissolved oxygen in September 1988 (Fig.27) is consistent with the salinity distribution (Fig.23b). High oxygen values around 150m coincide with the salinity maximum, the lowest oxygen values in the east coincide with the salinity minimum. The oxygen minimum zone at 150-500m appears to be isolated from the rest of the basin an unaffected by the intrusions of the Dardanelles lower layer. On the western side, the basin had been ventilated by intrusions to a depth of 300m forming a wedge extending eastwards. The stable layer with the minimum oxygen lay between wedges of relatively more oxygenated water. EBBESMEYER, BARNES and LANGLEY (1975) observed a similar structure in the Puget Sound, where there was a relatively static body of water opposite the mouth of the sound which remained depleted in oxygen for long periods of time, whereas in the rest of the sound the circulation was rapid. The deep oxygen maximum coincided with the temperature and salinity anomalies which resulted from deep renewals, and contained decreasing oxygen concentrations in the three deep depressions from west to east.

It is instructive to compare the behaviour of the water masses with the results of different measurements. The results of oxygen isotope measurements at a station in the east of the Marmara Sea which were carried out by SWART (1991) during the *Knorr* cruise to the Black Sea are illustrated in Fig.28. The Mediterranean water is characterized by $\delta_{18}O = 1.8$ppt. The upper part of the sub-halocline waters corresponding to the temperature maximum, and those below a depth of 350m have $\delta_{18}O$ values higher than the water between 150-300m. This implies that the renewal time of the waters at 150-300m depth of the Marmara Sea is higher than for the other parts of the water column.

CFC-11 measurements taken in the easternmost deep basin of the Marmara Sea, in June 1988 (BULLISTER, private communication) and in December 1993 (TANHUA and FOGELQVIST, private communication) are shown in Fig.29. Both profiles show saturation concentrations at the surface, with rapid decreases at the pycnocline and small variations further down. The two profiles are similar and the small differences between them could have resulted from there being about 5 years between measurements.

In the eastern deep basin of the Marmara Sea, CFC-11 measurements also show saturation at the surface, a decrease to 2pmol kg^{-1} below the pycnocline, and further decreases to a minimum value of 1pmol kg^{-1} at 200m. Below 200m, the CFC-11 values remain approximately constant down to 700m, but further down the concentrations increase to a maxima at 800m and 1000m, with a value of 1.8pmol kg^{-1}. The age of the water masses between the pycnocline and 700m is about 20 years and renewals with smaller age of waters occur only deeper than 800m. An immediate decrease from saturated surface values (4.4pmol kg^{-1}) to 2pmol kg^{-1} below the pycnocline shows a lack of mixing between the upper and lower layers of the Marmara Sea, and the big difference between their mean residence times.

At the western part of the basin, the CFC-11 profile exhibits a different shape (TANHUA and FOGELQVIST, unpublished data). The CFC-11 concentrations fall to a minimum value of 1.4pmol kg^{-1} at 300m but then increase to a value of 3pmol kg^{-1} at 600m, below which the concentration remains relatively constant. The water below 600m in the western part of the basin has recently been ventilated, whereas the water at about 400m has remained stagnant for some time.

When comparing the western and eastern parts of the basin, it is evident that in the west water below 600m has been renewed relatively recently, but in the eastern part, only below 800m has there been renewal by deep water flows from the west. While the apparent age of the renewed water is about 2 years in the western part, the apparent age of the youngest water mass in the eastern part is 10 years.

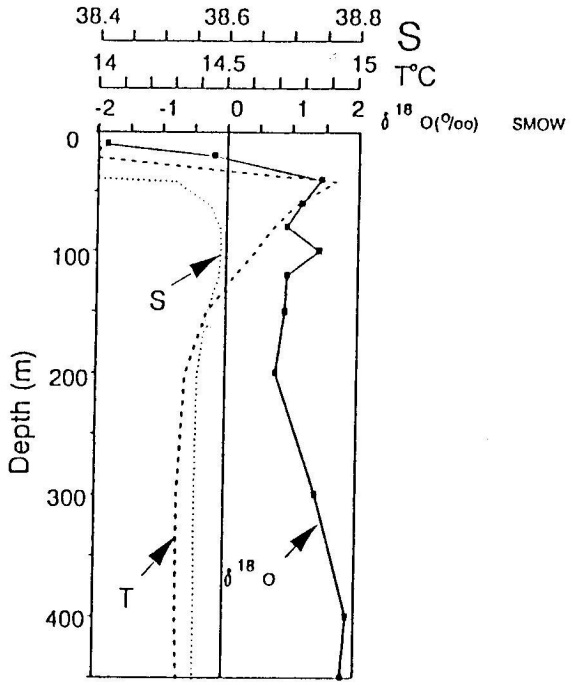


FIG.28. Profiles of temperature, salinity and $\delta^{18}O$ in the eastern deep basin of the Marmara Sea (Fig.3, SWART, 1991).

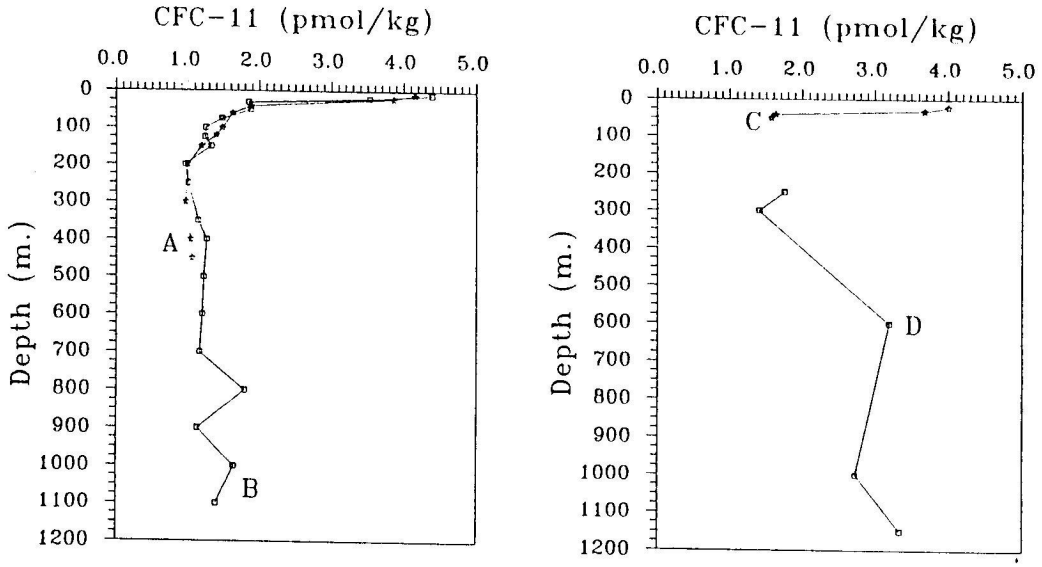


FIG.29. Vertical distribution of the CFC-11 in the Marmara Sea at (a) eastern basin and (b) western basin. Profile A obtained during the Knorr cruise in June 1988 (BULLISTER, personal communication) and pofiles B, C, D obtained in December 1993 (TANHUA and FOQELQVIST, personal communication.

7.3 Interior mixing

Intrusion of the Mediterranean water into the Marmara Sea occurs as a negatively buoyant plume which introduces temperature and salinity differences while maintaining the stability of the water column. Fine structure temperature and salinity anomalies are limited to the western part of the basin. There are indications that double diffusive instabilities could play important roles in vertical mixing, subsequent to the intrusions.

The mixing between water masses having different temperatures and salinities is characterized by the Turner angle related to the density ratio R_ρ (RUDDICK, 1983),

$$Tu = \frac{N_T^2 - N_S^2}{N_T^2 + N_S^2},$$

where $N_T^2 = g\alpha\delta_z T$, $N_S^2 = g\beta\delta_z S$, where α is thermal expansion coefficient, β is salinity contraction, T is the tempeature, S is the salinity, g is the gravitational acceleration and z is the vertical coordinate.

Turner angle (Tu) variations in the water column define the following classification of the stability of the layers.

$-90° < Tu < -45°$ diffusively unstable,

$Tu < 45°$ stable,

$45° < Tu < 90°$ finger sense unstable,

$Tu > 90°$ gravitationally unstable.

Turner angle profiles computed for two stations from the eastern and western part of the basin in March 1990 are given in Fig.30. Except in the upper 200m there are differences in stability and mixing characteristics between the eastern and western parts. A 'finger-sense' unstable region was observed at a depth of 150-200m which coincides with the interface between cold-less salty water beneath warm-salty water (cf Fig.20). The western basin appears to have various layers with double diffusive instabilities.

7.4 Circulation characteristics of the subhalocline waters

The pattern of the deep circulation of the sub-halocline water mass can be inferred from charts of the parameters on constant sigma-t surfaces, since, in the absence of mixing, a geostrophically balanced flow should be parallel to these surfaces.

Circulatory features of the sub-halocline waters are presented using the $\sigma_\theta = 28.82$ surface in September 1988 (Fig.31). The isolines show the eastward moving meandering current. Comparing this figure with the bottom topography of the Marmara Sea (cf Fig.1b), it is seen that perturbations in the flow, in the form of a trapped anticyclonic vortex, are strongly related to the sill between the western and central basins. A transect of sigma-t along the main axis of the Marmara Sea (Fig.32) shows that this feature extends to great depths, so the circulation of the deep waters of the Marmara Sea is constrained to follow isobaths and is therefore accentuated over the steeper parts of the topography.

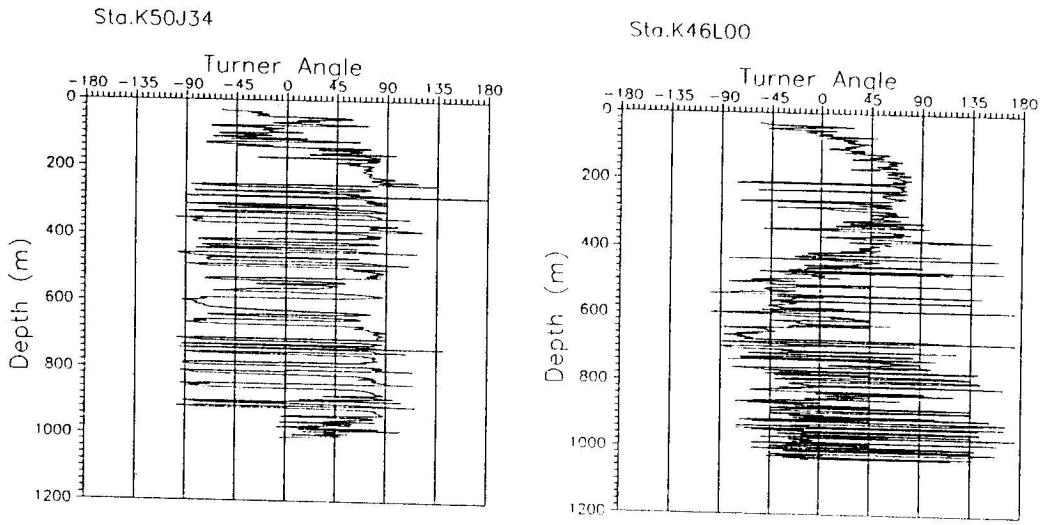


FIG.30. Turner angle profiles at March 1990 from two different stations.

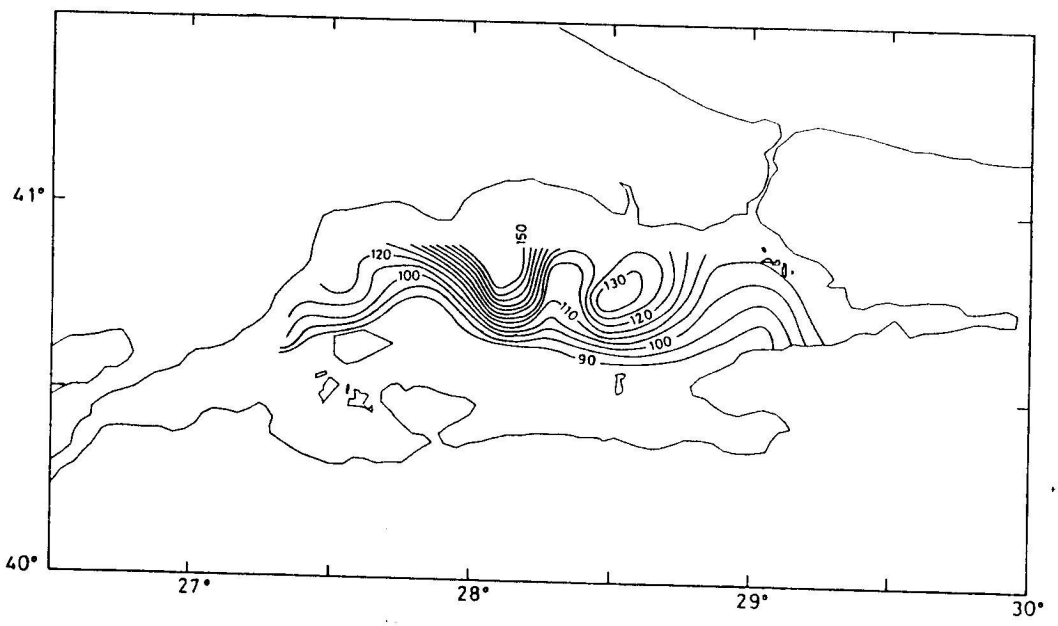


FIG.31. Depth of the sigma-t = 28.82 surface in September 1988.

As theoretically predicted by HUPPERT (1975) and later applied by LAGERLOEF (1983), the flow is influenced by topography when Rossby numbers are small and stratification is weak. For the deep waters of the Sea of Marmara, one expects the flow velocities to be low enough to keep the Rossby number small. Stratification in the water column is given by the stratification parameter (S) as:

$$S = \frac{ND}{fL},$$

where N is the Brunt-Vaisala frequency, D is the total fluid depth over the depression or bank, L is the length of the depression or bank and f is the Coriolis parameter.

The Brunt-Vaisala frequencies can be calculated using

$$N^2 = \frac{g}{\rho}\frac{\delta\rho}{\delta z}$$

where g is gravitational acceleration ($9.87ms^{-1}$), ρ is density, and z is depth.

Typical values for the bank between the western and central depressions are D = 750m, L = 20 x 10^3m, and f = 10^{-4}. Using the measured values given in Table 2, the stratification parameter is found to be between 0.3 and 1.0 for the sub-halocline part of the basin. These values confirm that S<O(1) and therefore that the water column stratification was sufficiently weak for the topographic influence on the flow to be important.

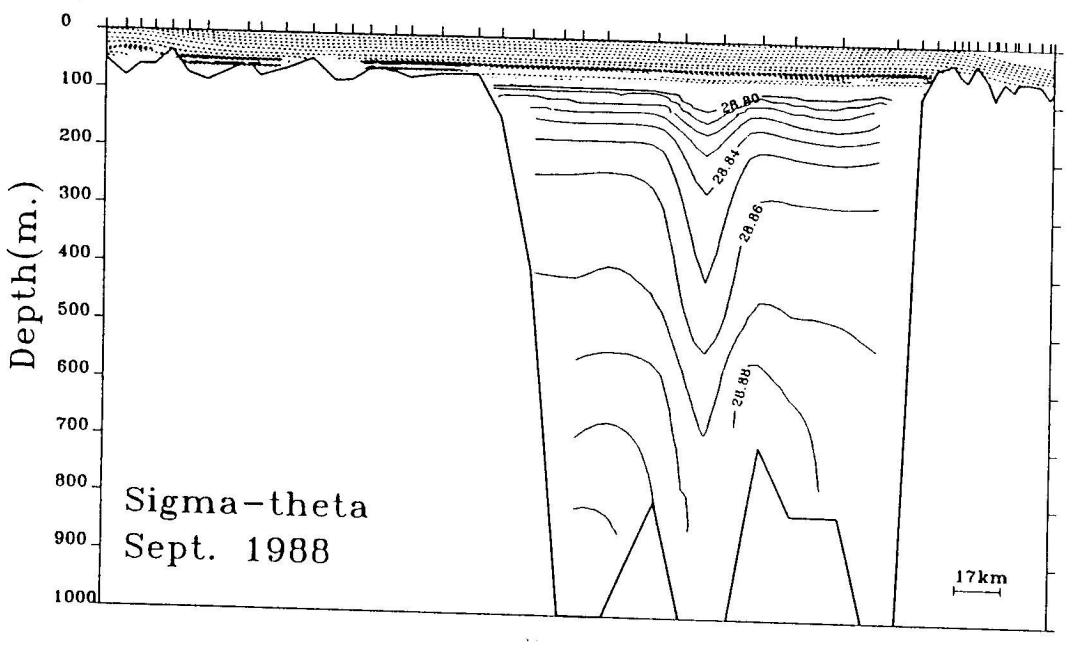


FIG.32. Sigma-theta transect from the Aegean Sea to the Black Sea along the main axis of the Marmara Sea in September 1988.

TABLE 2. σ_T values and corresponding parameters required for Brunt-Vasila frequency calculation at Station K50K00 in September 1988

σ_T (kgm^{-3})	Depth (m)	Δz (m)	N^2 (s^{-2})
28.75	53		
		31	0.0039
28.80	84		
		12	0.0028
28.81	96		
		16	0.0024
28.82	112		
		18	0.0023
28.83	130		
		29	0.0018
28.84	159		
		33	0.0017
28.85	192		
		73	0.0011
28.86	265		
		165	0.0007
28.87	430		
		135	0.0008
28.88	565		
		242	0.0006
28.89	807		

7.5 Outflow of the sub-halocline waters

The Bosphorus strait which has a minimum depth of 40m at its southern end, is the only exit for the outflow of sub-halocline waters so there is no vbarrier to the outflow of water from the Sea of Marmara down to 40m depth.

The behaviour of the water in the Bosphorus-Marmara Junction is illustrated by the cross sections along the axis of this submarine canyon in two different months (Fig.33a,b). In September 1989 (Fig.33a) the upward tilting of the isolines in the upper 125m near the Bosphorus indicates that the water from the interior was being sucked into the Bosphorus. However, when the Bosphorus upper layer was thinner, as in February 1989, the isopycnals were oriented towards the eastern wall of the basin instead of uplifting (Fig.33b).

These observations exemplify a well-known problem in fluid mechanics, the selective withdrawal mechanism. STOMMEL, BRYDEN and MANGELSDORF (1973) and recently KINDER and BRYDEN (1990) propsosed that such a mechanism occurs at the Straits of Gibraltar where lower layer flow towards the Atlantic is capable of sucking up deep Mediterranean water. In general, the requirements for such a mechanism are mild stratification in the interior and strong flow at the strait (KINDER and BRYDEN, 1990).

The Sea of Marmara also appears to meet these requirements in September whereas in the other seasons when the lower layer flow is expected to be weaker, either the water was being sucked from shallower levels than in September, or selective withdrawal was not occurring.

This removal of the water from the interior through the selective withdrawal mechanism is an environmentally important phenomenon, since the near-surface waters removed are recently intruded and possess higher oxygen concentration than waters in other parts of the interior. However, once the withdrawal effect reaches depths >125m, it begins to draw on the waters of minimum salinity and minimum oxygen content, which are the most stagnant in the Marmara Sea with the longest renewal time. So when the selective withdrawal mechanism is operating, it can be some of the oldest water which is being removed.

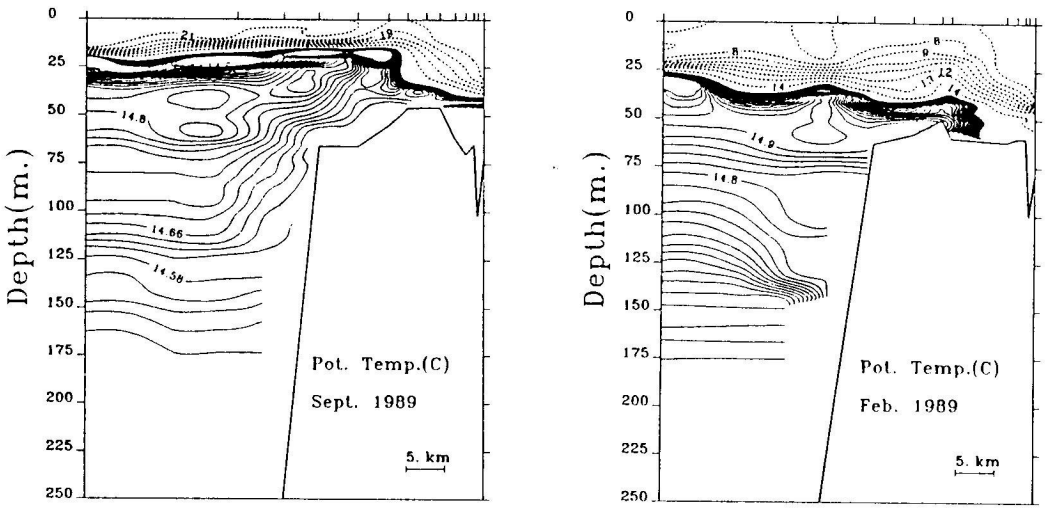


FIG.33. Potential temperature transect in and along the main axis of the Bosphorus (a) September 1989; (b) February 1989.

8. SUMMARY AND CONCLUSIONS

The observations we have presented describe the seasonality of the circulation and hydrography of the Marmara Sea.

During winter and spring the surface salinity is characterized by relatively high values over the whole Sea, as a consequence of wind-induced mixing and reductions in Black Sea discharge. During summer-autumn periods, surface salinities become relatively low as a result of lack of mixing between the upper and lower layers. Mixing of the sub-halocline waters into the upper layer occurs through two mechanisms: (a) the entrainment into the Bosphorus outflow and (b) wind mixing, which introduce equal amounts of water into the upper layer, but wind mixing is more effective in the southern part of the basin where the total depth is less than 200m.

The mean upper layer circulation in the Marmara Sea is a basin scale anti-cyclonic gyre which is driven mainly by the sea level differences between the Black Sea and the Aegean. This anti-cyclonic gyre is modified by the Bosphorus jet during the high outflow conditions (spring and early summer) and by the wind stress during the winter. These features of the upper layer circulation are illustrated schematically in Fig.34a.

Denser Mediterranean waters enter the Marmara Sea through the Dardanelles Strait in the form of a turbulent buoyant plume and form the subhalocline waters of the basin. The effects of basin topography and the seasonal variability of the inflow from the Dardanelles lead to the subhalocline waters of the Marmara Sea having a heterogeneous structure. The effects of the inflow are observed first and most clearly in the western basin. The sinking and spreading of the Dardanelles plume is strongly seasonal. During the winter it sinks to the bottom of the western basin where it creates temperature and salinity anomalies in the deep waters. The eastward movement of the intrusions

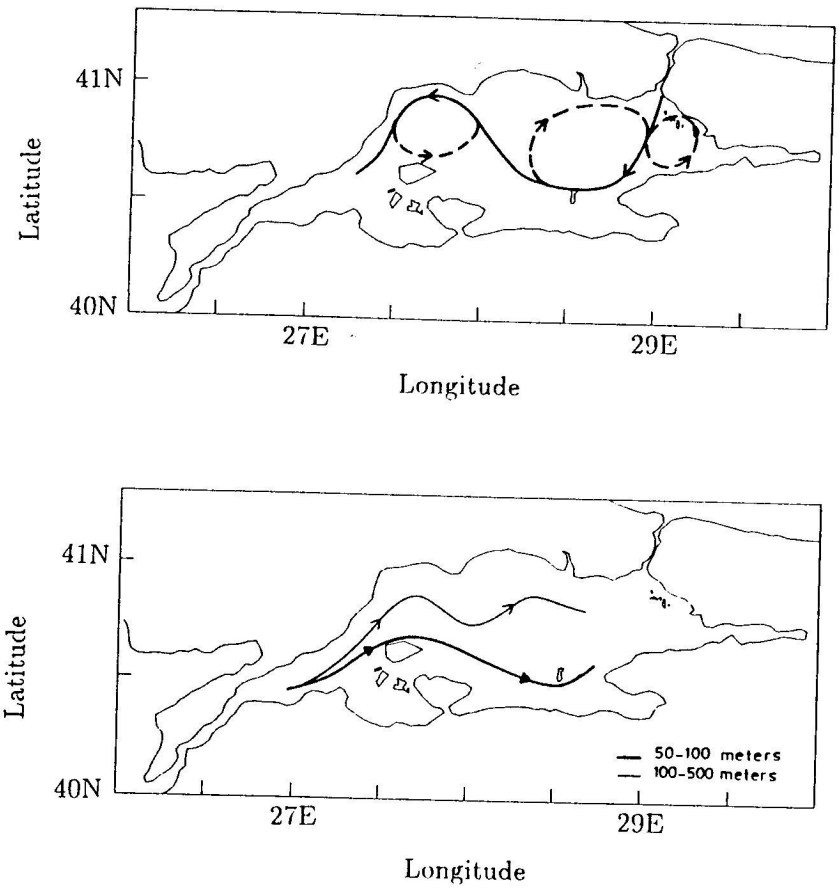


FIG.34. Schematic representations of the circulation of the Marmara Sea emerging from synthesis of the data collected during 1987-1992 period; (a) upper layer. Solid (dashed) lines indicate quasi-permanent (recurrent) features. (b) Sub-halocline circulation.

is restricted by the deep sills between the basins. In autumn the intrusions are seasonal and characterized by high temperature and high salinity anomalies immediately below the halocline. In some seasons the plume sinks to intermediate depths of 150-500m. In the eastern basin the water remains relatively stagnant over long periods of time, compared to the frequent renewal of the western basin. As a result, the minimum salinity and oxygen zone are more pronounced in the eastern basin. The circulation in the sub-halocline of the Marmara Sea is very slow, the net motion being a slow drift from west to east following the bathymetry. This circulation is shown schematically in Fig.34b.

Internal mixing processes occurring in the sub-halocline part involve the interaction between recently introduced waters with the interior water mass, and 'finger-sense' instability of the water column. While water mass mixing was seen to be quite active in the western part, in the eastern part the water remained quite stagnant. Existence of the warm-saline water above cold-less saline water was favouring the condition for 'finger-sense' unstability, resulting in the slow downward diffusion of the warm-saline waters observed.

9. ACKNOWLEDGEMENTS

We gratefully acknowledge the efforts of the captains and crew of R/V *Bilim* and our colleagues at the IMS-METU for collecting data. This study was supported by the Turkish Scientific and Technical Research Council as part of National Monitoring Programmes and by the Municipality of Istanbul, as part of the Studies performed for them in the Turkish Straits.

10. REFERENCES

AAGARD, K., J.H. SWIFT and E.C. CARMACK (1985) Thermohaline circulation in the Arctic Mediterranean Seas. *Journal of Geophysical Research*, **90(C3)**, 4833-4846.

ANDERSON, J.J. and E.C. CARMACK (1984) Observations of chemical and physical fine-structure in a strong pycnocline, Sea of Marmara. *Deep-Sea Research*, **21**, 877-886.

ARMI, L., and D.M. FARMER (1987) A generalization of the concept of maximal exchange in a strait. *Journal of Geophysical Research*, **83**, 873-883.

ARTÜZ, M.I. (1974) Hydrographic data for the Bosphorus and surrounding regions, for the period 1949-1973. Section II. *Hydrobiology Research Institute, Faculty of Science, University of Istanbul*, 154pp (in Turkish).

BAŞTÜRK, Ö., C. SAYDAM, I. SALIHOGLU and A. YILMAZ (1986) Oceanography of the Turkish Straits - First Annual Report, Vol.III, Health of the Turkish Straits II: Chemical and Environmental Aspects of the Sea of Marmara, Institute of Marine Sciences, METU, Erdemli, Içel, 86pp.

BAŞTÜRK, Ö., C. SAYDAM, I. SALIHOGLU and A. YILMAZ (1988) Oceanography of the Turkish Straits - Second Annual Report, Vol.II, Health of the Turkish Straits: Chemical and Environmental Sepcts of the Sea of Marmara and the Golden Horn, Institute of Marine Sciences, METU, Erdemli, Içel, 130pp.

BAŞTÜRK, Ö., C. SAYDAM, I. SALIHOGLU and A. YILMAZ ((1990) Oceanography of the Turkish Straits - First Annual Report, Vol.II, Health of the Turkish Straits: Chemical and Environmental Aspects of the Sea of Marmara, Institute of Marine Sciences, METU, Erdemli, Içel, 69pp.

BEŞİKTEPE, Ş. (1991) *Some aspects of the circulation and dynamics of the Sea of Marmara*. PhD Thesis, Institute of Marine Sciences, Middle East Technical University, Erdemli, Içel, 226pp.

BEŞİKTEPE, Ş., E. ÖZSOY and Ü. ÜNLÜATA (1993) Filling of the Sea of Marmara by the Dardanelles Lower Layer Inflow. *Deep-Sea Research*, **40**, 1815-1838.

BO PEDERSEN, F. (1980) *A monograph on turbulent entrainment and friction in two-layer stratified flow*. Series Paper No.**25**, Institute of Hydrodynamics and Hydraulic Engineering, Technical University of Denmark, 397pp.

BOGDANOVA, C. (1969) Seasonal fluctuations in the inflow and distribution of the Mediterranean waters in the Black Sea. In: *Basic Features of the Geological Structure, of the Hydrologic Regime and Biology of the Mediterranean Sea*, L.M. FOMIN, editor, Academy of Sciences, USSR, Moskow. English translation 1969 Institute of Modern Languages, Washington DC, 131-139.

BRODY, L.R. and M.J.R. NESTOR (1980) Regional forecasting aids for the Mediterranean Basin, Handbook for forecasters in the Mediterranean, Part 2, Naval Environmental Prediction Research Facility, Monterey, California, Technical Report TR80-10, 178pp.

BÜYÜKAY, M. (1989) *The surface and internal oscillations in the Bosphorus related to meteorological forces*, MSc Thesis, Institute of Marine Sciences, Middle East Technical University, Erdemli, Içel, 169pp.

DE FILIPPI, G.L., L. IOVENITTI and A. AKYARLI (1986) Current analysis in the Marmara-Bosphorus junction. *Ist AIOM (Associazione di Ingegneria Offshore e Marina) Congress, Venice, June 1986*. 5-25.

EBBESMEYER, C.C., C.A. BARNES and C.W. LANGLEY (1975) Application of an advective-diffusion equation to a water parcel observed in a fjord. *Estuarine and Coastal Marine Sciences*, **3**, 249-268.

FARMER, D.M. and L. ARMI (1986) Maximal two-layer exchange over a sill and through the combination of a sill and contraction with barotropic flow. *Journal of Fluid Mechanics*, **164**, 53-76.

GERTMAN, I.F., I.M. OVCHINNIKOV and Y.I. POPOV (1990) Deep convection in the Levantine Sea. *Rapports et Procès-verbaux des Réunions. Commission Internationale pour l'Exploration Scientifique de la Mer Méditerranée*, **32**(2), 172.

HUPPERT, H.E. (1975) Some remarks on the initiation of inertial Taylor columns. *Journal of Fluid Mechanics*, **58**, 517-537.

KINDER, T.K. and H.L. BRYDEN (1990) Aspiration of deep waters through straits. In: *The physical oceanography of sea straits*, L.J. PRATT, editor, NATO-ASI Series, 295-319.

LAGERLOEF, G. (1983) Topographically controlled flow around a deep trough transecting the shelf off Kodiak Island, Alaska. *Journal of Physical Oceanography*, **13**, 139-146.

LATIF, M.A., E. ÖZSOY, T. OĞUZ and Ü. ÜNLÜATA (1991) Observations of the Mediterranean inflow into the Black Sea. *Deep-Sea Research*, **38**, Suppl.2, 711-723.

LATIF, M.A., E. ÖZSOY, S. BEŞIKTEPE, T. OĞUZ and H.I. SUR (1992) Volume flux measurements in the Bosphorus using an acoustic doppler current profiler. *Rapports et Procès-Verbaux des Réunions. Commission Internationale pour l'Exploration Scientifique de la Mer Méditerranée*, **33**, 221.

LATIF, M.A., T. OĞUZ, H.I. SUR, Ş. BEŞIKTEPE, E. ÖZSOY and Ü. ÜNLÜATA (1990) Oceanography of the Turkish Straits - Third Annual Report, Vol.I. Physical Oceanography of the Turkish Straits, Institute of Marine Sciences, METU, Erdemli, Içel, 201pp.

LATIF, M.A., E. ÖZSOY, I. SALİHOĞLU, A.F. GAINES, Ö. BAŞTÜRK, A. YILMAZ and S. TUĞRUL (1992) Monitoring via direct measurements of the modes of mixing and transport of wastewater discharges into the Bosphorus Underflow. *METU - Institute of Marine Sciences*, Erdemli, Içel, Turkey, Technical Report No. **92-2**, 98pp.

MEE, L.D. (1992) The Black Sea in crisis: The need for concerted international action. *Ambio*, **24**, 278-286.

MOORE, W.S. and D.J. O'NEILL (1991) Radionuclide distributions in recent sea sediments. In: *The Black Sea Oceanography*, E. IZDAR and J.M. MURRAY, editors, NATO/ASI Series, Dordrecht, Kluwer Academic Publishers, 257-270.

MÖLLER, L. (1928) Alfred Merz' hydrographische untersuchungen in Bosphorus und Dardanellen, Veroffentlichungen des instituts für Meereskunde an der Universitat Berlin, Neue Folge A, **18**, 3-284.

NIELSEN, J.N. (1912) Hydrography of the Mediterranean and adjacent waters. In: *Report of the Danish Oceanographical Expeditions 1908-1910 to the Mediterranean and adjacent waters*, J. SCHMIDT, editor, Copenhagen, **1**, 72-191.

OĞUZ, T. and H.I. SUR (1989) A two-layer model of water exchange through the Dardanelles Strait. *Oceanologica Acta*, **12**, 23-31.

OĞUZ, T., E. ÖZSOY, M.A. LATIF, H.İ. SUR and Ü. ÜNLÜATA (1990) Modelling of hydraulically controlled exchange flow in the Bosphorus Strait. *Journal of Physical Oceanography*, **20**, 945-965.

ÖZSOY, E. (1990) On the seasonally varying control of the Black Sea exchange through the Bosphorus, *EOS*, **71**(2), 138.

ÖZSOY, E., M.A. Latif, S. Tugrul and Ü. ÜNLÜATA (1992) Water and nutrient fluxes through the Bosphorus, and exchanges between the Mediterranean and Black Sea, International Conference on Problems of the Black Sea, Sevastopol, Ukraine, 10-15 November 1992. In: *Problems of the Black Sea*, Mhiuas, 54-67.

ÖZSOY, E., T. OĞUZ, M.A. LATIF and Ü. ÜNLÜATA (1986) Oceanography of the Turkish Straits. *First Annual Report*, Institute of Marine Sciences, Middle East Technical University, Vol.**1**, 269pp.

ÖZSOY, E., T. OĞUZ, M.A. LATIF, Ü. ÜNLÜATA, H.I. SUR and Ş. BEŞIKTEPE (1988) Oceanography of the Turkish Straits. *Second Annual Report*, Institute of Marine Sciences, Midele East Technical University, Vol.**2**, 269pp (in Turkish).

ÖZSOY, E., M.A. LATIF, Ş. BEŞIKTEPE, T. OĞUZ, I. SALİHOĞLU, A.F. GAINES, S. TUĞRUL, Ö. BAŞTÜRK, C. SAYDAM, S. YEMENICIOGLU and A. YILMAZ (1992) Monitoring via direct measurements of the modes of mixing and transport of wastewater discharges into the Bosphorus underflow. Second Progress Report. METU-Institute of Marine Sciences, Erdemli, Içel, 310pp.

PEDLOSKY, J. (1987) *Geophysical Fluid Dynamics*, Springer Verlag, 710pp.

PEKTAŞ (1953) Surface currents in the Bosphorus and Sea of Marmara, *Publication of the Hydrobiology Research Institute, Faculty of Science, University of Istanbul, Hydrobiology Series*, **A**, v.1, no.4, 154-169 (in Turkish).

POLAT, Ç. and S. TUĞRUL (1994) Nutrient and organic carbon exchanges between the Black and Marmara Seas through the Bosphorus Strait. *Continental Shelf Research*, (in press).

RUDDICK, B. (1983) A practical indicator of the stability of the water column to double-diffusive activity. *Deep-Sea Research*, **30**, 1105-1107.

STANLEY, D.J. and C. BLANPIED (1980) Late quaternary water exchange between the eastern Mediterranean and Black Sea. *Nature, London*, **286**, 538-541.

STOMMEL, H., H. BRYDEN and P. MANGELSDORF (1973) Does some of the Mediterranean outflow come from great depth? *Pure and Applied Geophysics*, **105**, 879-889.

SUR, H.İ., E. ÖZSOY and Ü. ÜNLÜATA (1994) Boundary current instabilities, upwelling, shelf mixing and eutrophication processes in the Black Sea. *Progress in Oceanography*, **33**, 249-302.

SENGÖR, A.M.C., N. GÖRÜR and F. SAROGLU (1985) Strike-slip faulting and related basin formation in zones of tectonic escape: Turkey as a case study. In: *Society of Economic Paleontologist and Mineralogists Special Publication*, **37**, 227-264.

ÜNLÜATA, Ü. and E. ÖZSOY (1986) Oceanography of the Turkish Straits - First Annual Report, Vol.III, Health of the Turkish Straits I: Oxygen deficiency of the Sea of Marmara, Institute of Marine Sciences, METU, Erdemli, Içel, 81pp.

ÜNLÜATA, Ü., T. OĞUZ, M.A. LATIF and E. ÖZSOY (1990) On the physical oceanography of the Turkish Straits. In: *The Physical Oceanography of Sea Straits*, L.J. PRATT, editor, NATO/ASI series, Kluwer, 25-60.